MICROBIAL INFLUENCE ON THE ACCUMULATION OF PRECAMBRIAN AEOLIAN DEPOSITS (NEOPROTEROZOIC, VENKATPUR SANDSTONE FORMATION, SOUTHERN INDIA)

Giorgio Basilici[1,2]*, Marcus Vinicius Theodoro Soares[1], Nigel Philip Mountney[3], Luca Colombera[3]

[1]Geosciences Institute, State University of Campinas, Campinas, Brazil.

[2]Centro Regional de Investigaciones Científicas y Transferencia Tecnológica (CRILAR-CONICET), Entre Ríos y Mendoza s/n., 5301, Anillaco, La Rioja, Argentina

[3] Fluvial & Eolian Research Group, School of Earth and Environment, University of Leeds, Leeds LS2 9JT, UK

*e-mail: giorgio@unicamp.br

ABSTRACT

In many presently active aeolian systems, processes of sediment erosion, transport and deposition are markedly influenced by vegetation, which acts as an important sediment stabilising agent. Current sedimentary models for hyperarid continental settings devoid of vegetation and with adequate sand supply and wind force envisage intense aeolian activity, resulting in the construction of extensive aeolian sand-seas (ergs). During the Proterozoic, the Earth's surface was devoid of vegetation, yet ergs are not so common in Proterozoic continental successions. High water-table levels, and erosional reworking by fluvial or marine processes are recognised as possible factors that restricted accumulation and preservation of extensive Proterozoic aeolian systems. By contrast, Proterozoic biotic communities have traditionally been considered largely incapable of markedly influencing clastic sedimentary processes in continental settings. However, since it is now known that bacteria have colonised parts of the continental Earth's surface since the Palaeoarchean, a question arises as to whether such organisms might have exercised some control on aeolian processes via substrate stabilisation.

The Neoproterozoic Venkatpur Sandstone Formation (maximum age 709 Ma) is an aeolian depositional unit comprising small, isolated barchanoid and transverse dunes, and dry and damp sand sheet palaeoenvironments. Water-table-influenced aeolian sand-sheet deposits composed of thin sand layers that alternate with a suite of microbially induced sedimentary structures (MISS) provide evidence for fossilised bacteria. These strata record the interaction between microbial mats and aeolian depositional processes, which enabled the construction and accumulation of sand deposits. As microbial mats stabilised and provided plasticity to the depositional accumulation surface, they protected underlying (i.e. accumulated) aeolian deposits from possible wind erosion, reducing the possibility that these stored deposits could be recycled as lagged input to a downwind aeolian system.

The stabilising influence of the microbial mats enabled the accumulation of the aeolian deposits, resulted in a marked decrease in the availability of sand for aeolian transport, and hindered construction and accumulation of large aeolian bedforms. This depositional model highlights the significance of the microbial mats for controlling the depositional processes in Precambrian aeolian-dominated environment. Probably, this model may be applied to other pre-vegetated Earth continental environments.

Key words: Aeolian depositional systems; microbially induced sedimentary structures (MISS); Neoproterozoic; Venkatpur Sandstone Formation; India.

1. INTRODUCTION

Aeolian depositional systems develop where the carrying capacity of the wind, sediment supply and sediment availability conspire to enable aeolian construction (Kocurek and Havholm, 1993; Kocurek, 1999; Kocurek and Lancaster, 1999). Sediment supply commonly depends on processes acting in upwind non-aeolian sedimentary systems (e.g., fluvial, wave-dominated shoreline, deltaic or glacial systems), which transport the sediment to loci where the wind is able to entrain it and to commence downwind transport to a site of aeolian system construction. The availability of this sediment for aeolian transport depends on a host of factors: water-table position; presence, type and coverage of biogenic surface-stabilising agents, notably vegetation; presence of gravel, mud or other clastic detritus that might somehow act to retard entrainment of surface sediment by the wind; cementation of the surface sediment to form a chemical crust (Kocurek and Havholm, 1993; Kocurek and Lancaster, 1999; Rodríguez-López et al., 2014). In present-day sedimentary systems, one of the most important factors governing the availability of sediment for aeolian transport is the presence of vegetation (Kocurek and Nielson, 1986; Lancaster and Baas, 1998; Basilici and Dal Bó, 2014).

In Archean and Palaeoproterozoic continental depositional systems, alluvial fans and low-sinuosity braided rivers were common environments (Eriksson et al., 1998; 2005; Long, 2006). From the Mesoproterozoic, continental systems appeared with characteristics similar to those developed from the Phanerozoic to the present time: for instance, large aeolian systems (ergs) are recorded from the end of the Palaeoproterozoic (2.0-1.8 Ga) (Eriksson et al., 2005; Simpson et al., 2013; Abrantes et al., 2020), and high-sinuosity rivers, some with well-developed floodplains, seem to have been present (Ielpi, 2017, 2018; Santos et al. 2017; Ielpi et al., 2018). Notwithstanding, the absence of rooted vegetation on the Earth's surface during the Meso- and Neoproterozoic should have exerted a marked influence on the development of continental depositional systems (Davies and Gibling, 2012).

On the current Earth's surface, the stabilising influence of vegetation controls the intensity and the rate of weathering, and rates of sediment erosion, transport and deposition. The absence of the stabilising influence of vegetation during the Precambrian might suggest the development of continental sedimentary systems that differed considerably to those that post-dated the evolution of land plants (Davies and Gibling, 2012). Thus, it seems reasonable to believe that in the Precambrian, a bare land surface might have encouraged the mobilisation of sand-grade sediment by the wind and the construction and accumulation of large aeolian systems, which might be expected to develop in more widespread environments and climates than in post-vegetation landscapes. Yet, Precambrian aeolian successions are not as abundant as might be expected (Eriksson and Simpson, 1998; Simpson et al., 2004; Rodríguez-López et al., 2014). Moreover, compared to Phanerozoic examples, Precambrian aeolian successions tend to exhibit a less complex internal sedimentary organisation (Rodríguez-López et al., 2014). These authors accounted for these traits as arising in response to: (i) the presence of water at, near or above the topographic surface, which resulted in increased cohesion of sand-grade material to hinder aeolian sediment transport, (ii) fluvial or marine reworking of the aeolian sediments that restricted long-term sediment accumulation and preservation; and (iii) a failure to recognise aeolian successions in highly deformed meta-sediments that might comprise part of a highly fragmentary Precambrian geologic record. Biotic effects on the capacity to limit the availability of sand for aeolian transport have hitherto been considered insufficient to significantly impact processes of aeolian erosion, transport and deposition (Eriksson et al., 2005).

Geochemical data indicate that the first presence of life on the Earth's surface can possibly be dated to 3.8 Ga (Schidlowski, 2005; Astafieva, 2019). Geochemical and micromorphological evidence suggests that during the Archean microbial communities colonised the terrestrial environments in shallow-water (3.466 Ga - Westall, 2005; Westall et al., 2006) and also developed in palaeosols (2.6 Ga - Watanabe et al., 2000; 3.0 Ga - Retallack et al., 2016). One of the oldest-known erg palaeoenvironments, the Makgabeng Formation of South Africa (2.0-1.8 Ga) records different forms of microbially induced sedimentary structures (MISS) (Eriksson et al., 2000; Simpson et al., 2013).

Microorganisms most commonly occur in colonies, typically embedded in their mucilaginous extracellular polymeric substances (EPS) (Wacey, 2009). They can generate an organic adhesive envelope (biofilm), whose continuous growth can form a thick organic layer, commonly named a microbial mat, which covers the entire sedimentary surface (Westall et al., 2006; Gerdes, 2007; Wacey, 2009). In terrestrial environments, fine-grained sandy substrates are the preferred site of colonisation of these bacterial communities because the ground water can move up by capillary action, thereby providing the required sustained humidity for the development of the microbial community present on the surface (Noffke et al., 2001). These bacterial communities interact with fine-grained clastic sediments through five processes: (i) levelling, (ii) stabilisation, (iii) imprinting, (iv) microbial grain separation and v) baffling, trapping and binding (Noffke et al., 2001). In this way, they can build or modify sedimentary structures, generating forms known as microbially induced sedimentary structures, MISS (Noffke et al., 2001; Gerdes et al., 2000; Noffke, 2010).This study examines a sedimentary dataset from the Venkatpur Sandstone Formation, a Neoproterozoic aeolian-dominated unit, the deposits of which display sedimentary structures whose formation is interpretable as controlled by microbial organisms.

This paper seeks to identify and discuss the mutual influence of the water table and the biotic community in the construction and accumulation of the Venkatpur Sandstone Formation. The work addresses the following research questions: (i) Could Precambrian terrestrial biotic communities have developed sufficiently in aeolian sedimentary systems so as to control stages of construction and accumulation of the deposits? (ii) Why is the preserved sedimentary architecture of Precambrian aeolian successions (ergs) simpler? (iii) Why is of Precambrian aeolian successions less common than might be expected?

In answering these research questions, this study provides sedimentological details of unusual Precambrian erg succession and identifies the role of a biotic community in influencing the construction and accumulation of a pre-vegetation aeolian depositional system. Results describe the sedimentary structures that record the presence of microbial communities on the accumulation surface. The work discusses how and on what scale the biotic community influenced the construction and accumulation of a Neoproterozoic wind-dominated depositional system.

2. GEOLOGICAL SETTING AND STRATIGRAPHY

The Venkatpur Sandstone Formation is a stratigraphic unit formed within the Proterozoic Pranhita-Godawari Basin, located in Telangana State (SE India). The Venkatpur Sandstone Formation is the youngest unit of the Sullavai Group. This formation overlies conformably Proterozoic fluvial deposits with aeolian influence (Mancherial Quartzite Formation) and is itself overlain unconformably by Triassic sediments (Gondwana Supergroup) (Fig. 1). The maximum age of the formation is 709 Ma, as determined by radiometric dating of detrital zircon (Joy et al., 2015). The unit crops out along a series of hills oriented NW-SE for more than 100 km. In the study area, the exposed succession of the Venkatpur Sandstone Formation attains a maximum thickness of c. 300 m (Chaudhuri et al., 2012). The succession is exposed as part of a monocline within which beds dip at 15-20° towards N75-90°; there are no faults with significant throw (Fig. 1). The lithology of the study formation comprises very fine-grained sandstone to granulestone, but c. 90% of the sediments is fine- to coarse-grained sandstone. Chakraborty (1991) recognised that, from NW to SE, the overall depositional system varied from the deposits of barchan dunes through a widespread sand sheet to a marine coastal area. In the study area considered in this paper, Chakraborty (1991) described a depositional environment with a broad sand sheet with small zibars, ponds and sabkhas, with interspersed, sparse, small aeolian dunes.

3. METHODS

Detailed study for this research was undertaken through analysis of the NW part of the natural exposures of the Venkatpur Sandstone Formation located between the cities of Bellampalli and Mancherial (Fig. 1). Excellent outcrop exposures permitted small- and large-scale detailed analyses. Field-based data collection used the following methodological approach. (i) Detailed description of the small-scale lithofacies, including measurements of morphological features of bedforms (e.g. vortex-ripple deposits) by digital calliper. (ii) Millimetre-scale measurement and facies analysis of 15 stratigraphic sections each from 1.5 to 28 m thick. (iii) Drawings and photomosaics of eleven large 2D exposures revealing the stratigraphic architecture of the formation in vertical cliffs. (iv) Measurement of c. 250 bounding surfaces (i.e. dip-azimuth records) and/or geometrical parameters of the bed forms (i.e. inclination and dip direction of bedding surfaces, cross-stratification surfaces, and bounding surfaces between the architectural elements). All planar data relating to cross-strata and bounding surfaces were rotated with respect to an original palaeo-horizontal. The bedding surfaces of a horizontal-bedded sandstone architectural element (see below) were taken as reliable approximation of the palaeohorizontal.

Desk and laboratory analyses were performed according to the following methods. (i) Field drawings and photomosaic panels were analysed to define the distribution of lithofacies and architectural elements in five vertical cliffs. (ii) Thirty-five thin sections of sandstone were used to define the grain-size distribution, textural and petrographic features by point counting of at least 300 points for each sample. (iii) The same thin sections were used to identify and classify micro sedimentary structures. (iv) Fifteen quartz grains from a horizontally bedded sandstone architectural element, in the size range of 400 to 1100 μm, were randomly picked after boiling in a 15% hydrochloric acid solution, washing in a milliQ ultrasonic bath and sieving (cf. Vos et al., 2014). Using a scanning electron microscope (SEM - mod. LEO 430) in secondary electron imaging mode, the surface microtextures for each grain were described to recognise the mechanisms of transport and sedimentation of this material. Name and microtexture definitions have been adopted by Mahaney (2002) and Vos et al. (2014). (v) Eighteen samples of a horizontally bedded sandstone architectural element (see below) were examined with Scanning Electronic Microscope (LEO - Model 430I) to verify the occurrence of microorganisms and to describe their morphological and geochemical characteristics in EDX point spots and maps. To avoid contamination by present-day microorganisms, small specimens were cut from larger samples, cleaned in milliQ water in an ultrasonic bath, dried, immersed in alcohol and flamed for three minutes before being coated with Au for SEM observations. (vi) Quantitative analyses of total organic carbon were carried out in three samples from deposits of the horizontally bedded sandstone architectural element. The samples were subjected to the same treatment described in (v) to avoid present-day contamination. The samples were comminuted into particles less than 75 µm across and were treated with 10% (v/v) HCl to eliminate inorganic carbon. The TOC content was obtained by combustion at 1150 °C using a TOC analyser equipped with a solids module (HT 1300 - Multi N/C 2100, Analytik Jena) at the Laboratory of Geochemistry, Institute of Geosciences, University of Campinas. (vii) The original wave parameters (wave period and water depth) of a sandstone lithofacies formed by vortex ripples (see below) were assessed by measurement of grain size, crest wavelength and height, and application of the Airy wave theory, following the instructions of Immenhauser (2009). To define the pre-compaction height of the vortex ripples, the empirical relationship proposed by Sheldon and Retallack (2001) was used; this can be applied to palaeosols and rocks of nonmarine sedimentary origin (see Supplementary material 1 for parameters and method used).

4. RESULTS

4.1. General characteristics

The depositional units of the Venkatpur Sandstone Formation are organised as tabular beds, interlayered with single sets that are cross-stratified; the dominant colour is red, but thin white beds are also present in some lithofacies. The grain size varies from very fine sandstone to granulestone, with 90% of the succession being in the range fine- to coarse-grained sand; most of the grains are rounded or well-rounded. Single beds or laminae are characterised by moderately sorted to well-sorted sand grains. From petrographic analyses the sandstone is classified as a sublitharenite (Tab. 1). Three large-scale architectural elements are recognised (Tab. 2): (i) cross-stratified sandstone, (ii) planar-laminated sandstone, and (iii) horizontally bedded sandstone.

4.2. Cross-stratified sandstone

4.2.1. Description

This architectural element constitutes c. 40% of the thickness of the Venkatpur Sandstone Formation and is composed of simple sets of cross-stratified, red (7.5R5/6) or light red (7.5R7/6) sandstone, 0.2 to 5.5 m thick, commonly less than 1 m; rarely, two or three overlying cross-stratified sets are stacked. Within sets, foresets have a dip angle of 12 to 20° and are tangential to the underlying surface. Reactivation surfaces are present, but not common. The foresets are characterised by alternations of sandstone laminae: coarse-grained (1 to 20 mm thick), medium-grained (5 to 30 mm thick), and fine- or very fine-grained ($\leq$1 to 4 mm thick). Coarse-grained laminae form lenses less than 0.4 m long with straight and sharp top surfaces, and straight or concave-up erosional bottom surfaces (Fig.2A); they occur mostly on the upper parts of the foresets. Medium-grained sandstone laminae are the most abundant. Overall, they are structureless, although in some cases they show a crude inverse grading (Fig. 2B). They are more than 1 m long, and pinch out toward the toe of the cross stratification. Medium-grained sandstone laminae are dominant in the upper parts of the cross stratification, where they alternate with coarse- and, rarely, fine-grained laminae. Medium-grained sandstone laminae are also present on the tangential bottom of the foresets (Fig. 2C), where some display a crude inverse grading. Fine-grained laminae have been observed only in the middle and lower portion of the cross stratification (Fig. 2D) and pinch out toward the upper portion. These laminae, which are lighter coloured, have constant thickness along the foresets for more than 1 m and are parallel to each other. Fine- or very fine-grained laminae alternate with medium-grained laminae, appearing similar in form and texture to the pin stripe laminations of Fryberger and Schenk (1988). The vertical contact of fine-grained laminae to underlying or overlying medium- or coarse-grained laminae is sharp. However, in some cases, the fine-grained sandstone penetrates within the interstices of medium- or coarse-grained sandstone, forming a weakly gradual lower transition.

The bottom surface of the cross-stratified sets is, in general, a planar and sharp surface parallel to the stratifications of underlying units of horizontally bedded sandstone or planar-laminated sandstone architectural elements. At the small-scale of the outcrops, the erosional nature of this surface is not clear, except in cases where it is possible to observe the upwind or lateral termination of the cross stratification (Fig. 3). Occasionally, at the bottom of a cross-stratified set, it is possible to observe tangential foresets which progressively climb over a horizontal downwind portion that is itself composed of medium-grained sandstone arranged in thin layers, each up to 0.3 m thick (Fig. 4). The top surface of units of the cross-stratified sandstone is a planar and horizontal surface, which locally can be characterised by asymmetrical concave-up depressions, more than 1 m wide and up to 0.1 m deep, and by small steps that coincide with the foresets of the cross-strata (Fig. 2E). The erosional depressions are filled by planar parallel laminations of medium- and fine-grained sandstone and in some cases by sets with small cross-laminations.

In exposures more than 160 m long and oriented in the same direction as the foreset dips, the cross-bedded sets are observed to have lateral continuities in excess of the length of the outcrop without significant variation in thickness. The top and bottom surfaces of the cross-stratified sets are planar and parallel to the overlying and underlying bedding of horizontally bedded sandstone or planar-laminated sandstone architectural elements (Fig. 5). However, when the same sets are observed in outcrops approximately perpendicular to the foreset dip, they display a lenticular shape, 5 to >50 m wide, with concave-up bottom and flat top. Clear erosional lateral edges are observable at large and small scale where sets overlie horizontally bedded sandstone or planar-laminated sandstone architectural elements (Fig. 6).

Restored foreset dip directions of the cross-strata indicate relatively consistent (i.e. tight unimodal) dip directions toward the northeast (Fig. 7). These values are consistent with the data reported for the same cross-strata by Chaudhuri (1970) and Chakraborty (1991).

4.2.2. Interpretation

Three main aeolian stratification types (grain flow, grain fall and climbing translatent strata) are recognised in this architectural element, justifying the interpretation of these cross-stratified sets a having been generated by the lee-side migration of aeolian dunes (Kocurek and Dott, 1981). Grain-flow deposits form the medium- and coarse-grained laminae. Fine-grained components are interpreted as grain-fall deposits; their uniform thickness, parallelism and pinching out toward the upper portion of the foreset correspond to the description of grain-fall deposits for present and ancient dunes (Hunter, 1977a; Kocurek and Dott, 1981). Medium-grained sandstone laminae, abutted on the lower tangential portion of the foresets, are interpreted as climbing translatent strata.

The distribution of grain flow, grain fall and climbing translatent strata on the foresets, together with the overall geometry of the sets, allows for a qualitative deduction of the general dimensions of the formative dune bedforms (Hunter, 1977a; Kocurek and Dott, 1981). In large dunes (probably with height more than 10 m) grain-fall deposits dominate on the upper part of the slipface, where the middle and lower portions are dominated by grain-flow deposits. In dunes of modest size (between 1 and 10 m high), grain-fall deposits tend to on the lower portion of the slipface and can be easily preserved in the rock record. Very small dunes less than 1 m in height are commonly composed dominantly of climbing translatent strata. Most cross-strata of the Venkatpur Sandstone Formation display thin grain-fall deposits interlayered with grain flows in the middle and lower parts of the foresets. Moreover, the thickness of grain-flow deposits seems to have some proportional relationships with the height of the dunes. Kocurek and Dott (1981) displayed a plot where dunes less than 10 m of height have grain-flow deposits with a maximum thickness of 30 mm. Grain-flow deposits of the Venkatpur Sandstone Formation are less than 30 mm thick. Based on these considerations the original height of the dunes of this unit was likely less than 10 m (cf. Romain et al., 2014).

The original shape (form) of the dunes can be deduced based on analysis of their internal characteristics of the preserved beds. The dune-sets of the Venkatpur Sandstone Formation are in general characterised by a simple internal structure, with rare reactivation surfaces. In only a very few examples are overlying climbing cross-stratified sets present. Moreover, cross-strata show a relatively tight unimodal distribution of dip directions of the foresets. Barchan and transverse dunes are characterised by uniform dip direction of the foresets, although barchan bedforms commonly exhibit a marked lee-side plan-form curvature tending to give rise to a broader distribution of foreset dip directions (Lancaster, 1995; Pye and Tsoar, 2009). The deposits of transverse dunes tend to be uniform and laterally continuous tabular cross-stratified sets (e.g. McKee, 1966). The dunes responsible for generating the accumulated cross-stratified sets of the Venkatpur Sandstone Formation were likely to have been of barchanoid or relatively straight-crested transverse type (Rubin, 1987; Rubin and Carter, 2006).

Horizontal laminae of medium-grained sandstone, which characterise the downwind continuation of the foresets in the lower parts of sets can be interpreted as thin residual dry interdune deposits. The climbing of the tangential foresets over these horizontal laminae is interpreted as accretion of the interdune area during the dune migration (Fig. 4; cf. Mountney and Thompson, 2002).

4.3. Planar-laminated sandstone

4.3.1. Description

This architectural element constitutes c. 20% of the thickness of the formation and forms intervals that are each typically 0.2 to 5 m thick. These units commonly alternate with horizontally bedded sandstone architectural element. This planar-laminated sandstone is formed of two lithofacies: (i) discontinuous, parallel-laminated, medium- to coarse-grained sandstone and (ii) continuous, parallel-laminated, fine- and medium-grained sandstone.

(i) The first lithofacies (c. 80% of the element type by thickness) comprises alternating fine- to medium-grained (180-300 μm) and medium- to coarse-grained (350-600 μm) red (10R5/6) sandstone laminae. Fine- to medium -grained sandstone laminae are 1 to 4 mm thick and 0.15 to 1 m long; medium- to coarse-grained sandstone laminae are 1 to 9 mm thick and 0.05 to 0.6 m long. In some cases, the laminae display a gentle convex-up top, where the coarsest grains are concentrated (Fig. 8A). Coarse-grained laminae have sharp upper and relatively gradual lower boundaries with medium- to fine-grained sandstone. Thus, each fine- to medium-grained and coarse-grained sandstone couple forms a crude inversely graded layer, up to 15 mm thick (Fig. 8A). In general, the laminae are planar and parallel, horizontal or inclined at low-angle (less than 3°) (Fig. 8A). In some cases, these planar parallel laminae are interlayered with small flattened lenses that are 15 to 25 mm thick and 0.15 to 0.4 m long, which show low-angle inclined cross laminations composed of alternating laminae of fine- and coarse-grained sandstone (Fig. 8B).

(ii) The second lithofacies (continuous, parallel-laminated, fine- and medium-grained sandstone) constitutes c. 20% of the thickness of the element and is characterised by fine- and medium-grained laminae, locally with weak inverse grading, up to 10 mm thick and laterally continuous for more than 2 m (Fig. 8C).

These two lithofacies are organised in sets 0.1 to 0.8 m thick, where they alternate in vertical succession.

4.3.2. Interpretation

Discontinuous, parallel-laminated, medium- to coarse-grained sandstone can be identified as the deposits of granule ripples (Sharp, 1963). Fryberger et al. (1979) described similar lithofacies, which they named type "b", formed of bimodal poorly sorted fine-grained sandstone to granule, organised in flattened lenticular laminae or thin beds, discontinuous, commonly with coarse grains concentrated on the upper weakly convex-up portion. Fryberger et al. (1992) identified these structures as granule ripples and distinguished small and large granule ripples. Small granule-ripple deposits, when observed in section, are characterised by irregular and discontinuous horizontal bedding with alignment of coarse grains, which in some cases cover convex-up ripple forms. Large granule-ripple deposits have low-angle inclined cross stratification, represented by thin alternating laminae of fine-grained and coarse-grained sandstone (Lancaster, 1995; Qian et al., 2012). Most of the sandstone of this lithofacies corresponds to small granule ripples (Fryberger et al., 1992). The lenses with cross lamination can be related to large granule ripples (cf. Mountney and Russel, 2004; 2006; 2009).

Continuous, parallel-laminated, fine- and medium-grained sandstone coincides with the subcritical climbing translatent strata of Hunter (1977b), as testified by thin and continuous laminations and by the presence of weak inverse grading.

Granule ripples originate via alternating processes of deposition and erosion; in some cases they develop by deflation of sand-dominated wind ripples to leave a coarse-grained lag; these types do not show evidence of accumulation via climbing, but seem to be forms "frozen" in situ

(Fryberger et al., 1979; Kocurek, 1981). In general, these structures signify a low availability of sand and/or a wind flow that was undersaturated with respect to its potential sand-carrying capacity. By contrast, climbing translatent strata form by continuous deposition of wind ripples in relatively uniform winds, saturated or supersaturated in sand (Fryberger et al., 1979; Kocurek, 1981). The common occurrence of granule-ripple deposits in this architectural element indicates the variable strength of the wind and a generally low availability of sand.

4.4. Horizontally bedded sandstone

4.4.1. Description

Horizontally bedded sandstone comprises c. 40% of the thickness of the Venkatpur Sandstone Formation and forms intervals that are 0.1 to 8 m thick. Horizontally bedded sandstone is formed of four lithofacies: (i) planar or irregular horizontal bedding, (ii) small planar-concave lens of medium-grained sandstone, (iii) sets with weakly undulated and irregular cross-strata, and (iv) symmetrical ripples.

(i) Planar or irregular horizontal bedding types are the most common lithofacies of this element. They constitute more than 90% of the entire architectural element and form vertically continuous intervals 0.06 to 1 m thick (Fig. 9A). This lithofacies is laterally continuous for more than 50 m. Planar or irregular horizontal beds are composed internally of couples of alternating coarser and finer layers of sandstone. At large scale the laminae appear planar, but when viewed up close some of these appear irregularly or undulose. Coarser layers are <1 to 60 mm thick, are 0.2 to >2 m in lateral continuity and are composed of well- to moderately sorted, white (5Y8/1 or N9) medium- or fine-grained sandstone with subangular to well-rounded clasts; coarse sand grains may be present. The frequency distribution of surface microtextures of fifteen selected sand grains from the coarser layer of this lithofacies is shown in Figure 10A. In decreasing order of frequency of occurrence, the following microtextures were observed: rounded outline, low relief, upturned plates, bulbous edges, elongated or equidimensional depressions, crescentic percussion marks, meandering ridges, graded arcs, silica pellicles, arcuate, circular and polygonal cracks and solution crevasses. Figure 10B-D displays the most common microtextures, as described in the figure captions. Fine- or very fine-grained sandstone layers are formed by well-sorted, light red (7.5R7/6) or red (7.5R5/6) sandstone with angular to subangular clasts and are 1 to 40 mm thick and 0.5 to >2 m in lateral continuity. Medium- and fine- or very fine-grained couplets form a weakly graded layer with sharp bottom and top (Fig. 9B). The chromatic differentiation is related to the presence of quartz cement with a thin film of clay smectite around the clasts in medium- or fine-grained sandstone and iron oxides or hydroxides and clay cement in fine- or very fine-grained sandstone (Fig. 9B). In general, medium-grained layers are structureless, but the thicker layers display delicate planar parallel alternations of medium- or fine-grained and coarse-grained sandstone, less than 20 mm thick and up to 1 m long (Fig. 9C); some examples display crude inverse grading. Moreover, in the thicker layers, the following features can be present: (i) small flattened and structureless lenses of coarse-grained sandstone, 4 to 10 mm thick and 40 to 80 mm long; (ii) small sets, 6 mm thick, with low-angle inclined cross lamination (Fig. 9C). Fine- or very fine-grained layers display numerous elongated grains with the long-axis orientated parallel to the bedding surface (Fig. 9D). In some cases, iron oxide or hydroxide cement, typical of these layers, shows a greater concentration to the top of the layer (Fig. 9B).

Planar or irregular horizontal beddings display tabular shape and lateral continuity for more than 2 m. Their top is generally planar, but in thin section small, irregular crests that are 2 to 4 mm high and 12 to 20 mm in spacing can be observed. Irregularly undulating laminae are characterised by variation in thickness and common lateral interruptions (Fig. 9A and E). The undulations form small domes or narrow anticlines (Fig. 9A); in some cases, more contorted laminae can be observed (Fig. 9E). Small domes and narrow anticlines are aligned along the same bedding surface and are typically 6 to 20 mm high and 30 to 40 mm wide, though in rare cases can be 50 mm in high and 80 mm wide; their spacing is irregular, varying between 40 and 140 mm (Fig. 9E and 11A). The external margins of the domes or narrow anticlines are composed of a fine-grained sandstone layer, whereas disorganised patches of medium-grained sandstone form their nucleii (Fig. 11A). In a few cases, the apical portion (crest) of some domes is ruptured (Fig. 11B). Horizontal laminae of alternating fine- or very fine- and medium-grained sandstone onlap the upturned margins of the domes and narrow anticlines (Fig. 11A). On the bedding surfaces these structures are rarely visible. Where evident, they appear as dissected curved bands, 9 to 25 mm wide, showing a chaotic distribution of fine- and medium-grained sandstone.

On the upper surfaces of some fine- or very fine-grained sandstone layers, small contiguous domes with circular or subcircular form can be observed; their diameter is 3 to 28 mm and their height is 1 to 2 mm; no internal structures are visible in section (Fig. 11C). In some cases, these structures can be observed on the crests of symmetrical ripples (Fig. 11D).

(ii) Small planar-concave lenses of medium-grained sandstone and sets with weakly undulating and irregular cross-strata constitute less than 5% of thickness of this element and are interlayered with planar or irregular horizontal beds. In section, it is relatively common to observe small planar-concave lenses of medium-grained sandstone, 1 to 3 mm thick, 2 to 7 mm wide and spaced 3 to 30 mm along the bedding surface. These lenses are completely encased by fine-grained sandstone (Fig. 11E) and on the bed surface they are associated with small asymmetrical ripples with sinuous crests, 1 to 2 mm high, 4 to 6 mm wide and $\leq$13 mm spacing (Fig. 11F). The medium-grained sandstone lenses occur just below the troughs between the ripples, whereas the ripple crests are themselves composed of fine-grained sandstone (Fig. 11F).

(iii) Sets with weakly undulating and irregular cross-strata constitute tabular or lenticular beds, 20 to 70 mm thick, characterised by irregular and weakly undulating foresets of alternating medium- and fine-grained sandstone with dip angles of 15 to 17° and angular bottoms (Fig. 12A).

(iv) Symmetrical ripples constitute less than 5% of the thickness of this element. They can form intervals 0.02 to 0.2 m thick, commonly interlayered with planar or irregular horizontal beds. Their lateral extent varies between 2 to >60 m. On the bedding surface, this lithofacies displays symmetrical ripples of fine-grained sandstone (125-177 μm), regularly spaced with narrow, in some cases bifurcate, crests (Fig. 12B). The decompacted mean height of these bedforms (determined using the formula of Sheldon and Retallack, 2001; see Supplementary material 1) is 6 mm. The mean spacing is 31 mm; the mean vertical form index (or ripple index) is 5.24; and the mean ripple symmetry index is 1.09. In section, these symmetrical ripples are characterised by cross laminations that symmetrically overlie the two sides of the bedform with a vertical angle of climb (i.e. pure vertical aggradation; Fig. 12C). On the bedding surface, it is relatively common to observe two different generations of symmetrical ripples, where the second generation overlaps the previous without disrupting it (Fig. 12D).

4.4.2. Interpretation

The interpretation of the lithofacies of the horizontally bedded sandstone is divided in two parts: (i) sedimentary structures produced by physical and biological processes, and (ii) sedimentary structures produced exclusively by physical processes.

4.4.2.1. *Sedimentary structures produced by physical and biological processes*

Most of the horizontally bedded sandstone architectural element consists of thin graded layers of couplets of medium- or fine-grained to fine- or very-fine grained sandstone, divided by horizontal and sharp surfaces, which do not show evidence of erosion. Gerdes and Krumbein

(1987), Gerdes et al., (1991), Noffke et al. (1997, 2001) and Bouougri and Porada (2007) described similar layers as biolaminites. Biolaminites are few millimetres thick, laterally continuous for decimetres, alternations of medium- to fine-grained sands or fine-grained sand to silt, whose deposition is associated with an interaction between physical and biological processes. Noffke et al. (1997) described present-day biolaminites in supratidal environments, where the thin graded layers are deposited by tidal effect. Between clastic depositional events, the bacteria community colonizes the accumulation surface generating a microbial mat, which protects and stabilises the finer sediment, thereby protecting it from possible erosion by wave or tidal processes. Noffke et al. (1997) even alleged that elongated grains of the upper finer portion have their long axes arranged parallel to bed stratification because, being enveloped by soft organic matter, which decreases the friction between them, they lay down horizontally according to the gravity.

The thickness, lateral continuity, grading, grain size, internal structures and sharp contacts of the thin layers described as planar or irregular horizontal bedding are very similar to biolaminites described by Noffke et al. (1997, 2001) and Bouougri and Porada (2007). This biolaminites correspond to the microsequences described by Noffke et al. (1997) and Noffke (2010). The fact that evidence of bacteria microfossils and organic matter (see description below) is found exclusively within the fine- or very fine-grained layers reinforce this interpretation. Moreover, the oxides or hydroxides that cement these fine- or very fine-grained portions may be attributed to the oxidation of pre-existing reduced minerals produced by the anaerobic decay of the organic matter (Eriksson et al., 2007).

Nevertheless, even though it is possible to compare the planar or irregular horizontal bedding with the biolaminites described by Noffke et al. (1997, 2001) and Bouougri and Porada (2007) from a palaeobiological perspective, the primary depositional processes recorded in Venkatpur Formation arise from a different set of physical mechanisms. The biolaminites described by the above cited authors were developed in tidally influenced environments. By contrast, the Venkatpur Sandstone Formation is an aeolian-dominated depositional environment (Chakraborty, 1991). The lower (coarser) portion of the layer of biolaminites is characterised by well-sorted texture, rounded grains and, in the thicker layers, by inversely graded laminae, pin-stripe laminations and low-angle cross laminations, suggesting deposition of climbing wind ripples (Fig. 9C and 13A) (Hunter, 1977b). Surface microtextural features of the coarser sand grains of this layer also suggest an aeolian origin for these sediments. Grains with rounded outlines, low relief, upturned plates, bulbous edges, elongated or equidimensional depressions and crescentic percussion marks, which are the most frequent textural features observed on the grain surfaces, are considered typical of aeolian desert sands (Margolis and Krinsley, 1974; Krinsley et al., 1976; Krinsley and Trusty, 1985; Costa et al., 2013; Vos et al., 2014). Even the other less common microtextures (meandering ridges, graded arcs, silica pellicles, arcuate, circular and polygonal cracks and solution crevasses) form in settings dominated by wind transport (Krinsley and Donahue, 1968; Krinsley et al., 1976; Mahaney, 2002).

The finer upper portion may have been accumulated by an interaction between aeolian and biological processes. Bacteria secrete an adhesive substance - EPS (Extracellular Polymeric Substance) - and some species have filaments, which act to baffle, trap and bind the wind-transported small grains that pass on the microbial-mat surface (Noffke et al, 2001; Gerdes, 2007; Wacey, 2009). This process permits aggradation on and within the microbial-mat layer; the fine-grained sand to silt transported by weak winds progressively form the finer portion of the biolaminations (Fig. 13B and 13C). Successively, more energetic winds deposited coarser grains on the previous layers but without eroding the fine- or very fine-grained sand because of the stabilising action of the microbial mat.

As discussed next, other sedimentary structures found in the horizontally bedded sandstone architectural element, can be related to MISS: petee, sand stromatolites and palimpsest ripples.

Petee. The presence of laminae of medium- to very fine-grained sandstone, which onlaps the upturned margins of the small domes and narrow anticlines means that these structures constituted topographically elevated forms on the bedding surface before the burial. This excludes the interpretation of these structures as postdepositional deformation structures (Collinson and Mountney, 2019). Moreover, these structures cannot be confused with physical bedforms (e.g. vortex ripples), because they lack any regular form and spacing and they do not possess internal structures. Efflorescence salt crusts on a flat surface can produce similar structures associated with surface deformation, called polygonal deformations, which in vertical section appear as bowl-shaped patches (Smooth and Castens-Seidell, 1994; see their Figs. 7B and 11). However, polygonal deformation differs from the features described here in three ways: (i) they are typical of muddier sands; (ii) they display regular spacing in vertical section; and (iii) the scale of deformation is commonly larger (from tens of centimetres to several metres). Possibly, these structures are petees, i.e. structures produced by the destruction of microbial mats. Petee is a term used by Gavish (1985), Reineck et al. (1990) and Gerdes et al. (1994) to define undulating, sometimes ruptured, ridges produced by gases or water trapped behind microbial films, which cause pressure on the underside of relatively impermeable microbial mats, causing them to become distorted. In the described examples, the distortion effects of the gases or water is demonstrated by the disorganised patches of sandstones just below the small domes or narrow anticlines (Fig. 11A). Significantly, the general absence of clay indicates that the sealing property of the fine-grained sandstone laminae, which cover the small domes or narrow anticlines, was most likely due to the presence of a relatively impermeable layer generated by the microbial mats. Finally, the structures described here are very similar to those illustrated by Gehling (2000; his Figs. 7A and B) in the terminal Proterozoic of the Ediacara Member and interpreted as petee.

Sand stromatolites. The small domes, unevenly distributed on the bedding surface, (Fig. 11C) are comparable with sand stromatolites, associated with localised bacterial communities that baffled, trapped and bound sand grains. These forms grow a few millimetres above the accumulation surface (Bottjer and Hagadorn, 2007; see their Fig. 4(a)-14B and C). Alternatively, these structures can be interpreted as microbial mat chips that ripped off and casually distributed on the depositional surface, on which they successively accreted. The interpretation of these structures as "adhesion warts" (Reineck, 1955 and Kocurek and Fielder, 1982) is unlikely because such features should be uniformly distributed on the bedding surface. In addition, Goodall et al. (2000) recognised that "adhesion warts" can be produced by several processes and recommend abandoning this term.

Palimpsest ripples. Wave ripples characterised by crests with different orientation (Fig. 12C) are commonly called interference ripples (Collinson and Mountney, 2019). However, when the dimensions of the two sets of ripples are similar, it is conceivable that the earlier set of ripples was protected from erosion by the waves that generated the second set of ripples. This protection was likely realised by microbial mats that covered the first generation of wave ripples. This type of MISS is named palimpsest ripples (Schieber, 2004).

In summary, planar or irregular horizontal beds are constituted of biolaminites. Irregular forms can be due to contraction, expansion and destruction of the microbial mat possibly relating to variations in the humidity conditions at or close to the accumulation surface and/or to the gas production by decay of the organic matter (Eriksson et al., 2007).

4.4.2.2. Sedimentary structures produce exclusively by physical processes

In this architectural element, sedimentation via aeolian processes is demonstrated by (i) sets with weakly undulated and irregular cross-strata and (ii) small planar-concave lens of medium-grained sandstone. . Sets with weakly undulated or irregular cross-strata (Fig. 12A) correspond to the adhesion ripples described by Kocurek and Fielder (1982), which are associated with the formation and climbing of wind ripples on a damp (or sticky) surface. Small planar-concave lenses of medium-grained sandstone (Fig. 11E) are associated with the formation of adhesion ripples, which did not undertake significant upwind aggradational climbing. Small medium-grained sandstone lenses, where observed on bedding surfaces, correspond to the troughs of small adhesion ripples, whose crests are formed by the adjacent fine-grained sandstone (Fig. 11F).

Symmetrical ripples (Fig. 12B and C) are interpreted as supercritical climbing sets of wave ripples (Allen, 1982; Collinson and Mountney, 2019), as their morphological characteristics are compatible with a genesis of oscillatory flows. Their trochoidal form and the vertical form index (or ripple index) values between 3.1 and 6.4 (mean value 5.24) justify the affinity of these wave ripples to vortex ripples (Bagnold, 1946; Allen, 1979; Allen, 1981).

4.5. Microfossils and organic-carbon content

Description

Microfossils were found exclusively within the fine- to very fine-grained red sandstone layers of horizontally bedded sandstone, which are interpreted as biolaminites. Preserved microfossils are in general isolated, but in some examples they form small colonies. They appear in the following forms: filaments, coccoids, rods, sheaths and extracellular polymeric substance (EPS).

Filaments. Filaments have cylindrical form, sometimes they are sinuous, frayed, broken in some portions and show striae lengthwise (Fig. 15A to C). Their lengths are more than 100 μm and their diameters range 2 to 5 μm. Filaments occur isolated and rarely with coccoids.

Coccoids. Coccoids are spherical forms with diameter 2 to 10 μm, probably suggesting different species. They are observed in small colonies or isolated (Figs. 15 D to F and 16A). In general, the external surface is smooth, but in some cases appears as deflated and can show small wrinkles. Astafieva (2019, her Pl.1, Fig. 7) described similar coccoid forms with diameter of 10 μm in Archean strata of Central Karelia (Russia).

Rods. Few microforms correspond to rods. They are 1 to 2 μm wide and 2 to 4 μm long. In some instances, two rods linked and attached to each other at their extremity are observed (Fig. 16 B).

Sheaths. Sheaths are less common tubular and hollow forms, 30 to 75 μm long and 1.9 to 5 μm wide. The wall of the sheath can exhibit small holes and part of the tubular form can appear deformed and squashed; forms show a wrinkly superficial texture (Fig. 16C).

EPS (*extracellular polymeric substance*). An extensive material covering, coating and enveloping the microorganism fossils may be interpreted as EPS. Its surface is slightly crinkly, granular or smooth, and may exhibit small holes (Fig. 16D).

EDX (electron diffraction X-ray spectrometry) spot analyses of the filaments and coccoids indicate occurrence of Si, O and C in the microphotograph area (Figs. 15C and 16A). Carbon mapping clearly displays a concentration of C in association with the microfossils (Figs. 15B and F).

Total organic-carbon measurements were carried out in three samples of fine-grained sandstone laminae of planar or irregular horizontal bedding, the same samples where microfossils were observed. The three TOC content, expressed as C, were 0.058 g/100g, 0.048 g/100 g, and 0.068 g/100 g. These values fall within the detection and quantification limits, and for this reason, are better considered as semi-quantitative.

Interpretation

The identification of the microfossils followed two principles: (i) the biological origin of the observed microorganisms and (ii) the compatibility of the interpreted depositional system with the occurrence of microorganisms (Westall et al., 2006).

The filaments can be attributed to bacteria with spiral form (Spirillum type) (Wacey, 2009). Frayed and broken filaments and lengthwise striae can be associated to degradation and shrinkage after cell death due to the lost of internal cytoplasm (Westall et al., 2006). The C distribution along the filaments suggests the organic origin of these microforms (Fig. 15B) and the EDX spot analysis indicates the presence of C. The spherical forms can be attributed to bacteria of the type coccus. Deflated forms and wrinkly surfaces can be associated with the post mortem fossilisation of the microorganism, when the cytoplasm was almost completely lost and the internal part of the cell was hollow (Westall et al., 2006). Also in this case, the EDX mapping distribution of the C (Fig. 15F) and the EDX spot analysis (Fig. 16A) show the organic origin of these forms. The rod shaped microfossils may be bacteria known as bacilli. The two rod forms attached to their extremity (Fig. 16B) demonstrate a living aspect: an almost complete cell division of two cells separated by a small "neck". Sheaths can be attributed to the action of bacteria colony, which during life formed an "envelope" composed of extra-polymeric substances (EPS), whose function was probably to protect the colony (Wacey, 2009). Living aspects of these microforms are demonstrated by plastic deformation and deflating of the sheath as well as by its wrinkly external microtexture (Fig. 16C), which are consequence of the death and degradation of the internal cytoplasm of the bacteria. The structures described above as EPS (Figs. 15E and 16B and D) are very similar to analogous forms described by Westall et al. (2000, 2006), and can thus be attributed to bacterial activity.

The microfossils have been observed in sandstone showing MISS (biolaminites and petee) and are associated with lithofacies formed in the presence of water (adhesion ripples and vortex ripples). These lithofacies testify to deposition in an environment where the capillary fringe was close to sedimentary surfaces and/or precipitation (rainfall) or flooding was common. Presence of water, light and an adequate fine- or very fine-grained sandy substrate constituted the ideal conditions for the colonisation of microbial communities and the development of microbial mats.

The TOC measurements showed that detectable amounts of organic C are present within the fine- or very fine-grained sandstone laminae of the planar or irregular horizontal bedding. Thus, the organic C may be associated with the bacteria activity that indirectly caused the deposition of these finer laminae.

4.5. Bounding surfaces of the architectural elements

Cross-stratified sandstone, planar-laminated sandstone and horizontally bedded sandstone are three architectural elements that occur inter-layered vertically (Fig. 14). Their vertical transitions always occur across sharp surfaces; in lateral view, they show considerable continuity for more than 160 m, which is the maximum width of the exposures (Fig. 5 and 6). The characteristics of these bounding surfaces depend on the orientation of the section and on the type of architectural element.

The bottom of the cross-stratified sandstone element is a flat and horizontal surface where observed in section parallel to the dip direction of the cross-strata (Fig. 5). But where this same bounding surface is observed in sections perpendicular to the cross-stratification dip direction, it takes the form of a concave-up surface, clearly erosional on the underlying horizontally bedded sandstone or planar-laminated sandstone elements (Fig. 6). This surface can be visualised in three dimensions as an elongated and slightly concave-up depression, from 5 to more than 50 m wide, over 160 m long in the same direction of the foreset dip, and from 0.4 to 2 m deep. The top surface of elements of cross-stratified sandstone is a horizontal erosional surface, parallel to the stratification. This surface is clearly erosional because it cuts the cross stratification (Fig. 3) and because, at small scale, erosional depressions with centimetric relief are clearly visible (Fig. 2E). In sections parallel or perpendicular to the foreset dip direction, the bounding surfaces of the other two architectural elements are sharp, parallel to the stratification surfaces and more than

160 m long (Figs. 5 and 6). No evidence of erosional processes is clearly observed at the contact of these surfaces.

The bounding surfaces that delimit the three architectural elements are first order surfaces (*sensu* Brookfield, 1977). Other lower-order bounding surfaces can be observed within each architectural element. In elements of cross-stratified sandstone, surfaces that indicate reactivation or rarely separate sets of cross stratification occur. In elements of planar-laminated sandstone, horizontal or low-angle, planar and erosional surfaces delimit sets of wind-ripple strata. In elements of horizontally bedded sandstone, surfaces that are sharp (but not erosional), planar and parallel to the stratification surfaces indicate the transition between planar or irregular horizontal bed and wave-ripple lithofacies.

5. DISCUSSION

5.1. Depositional system

The cross-stratified sandstone represents an aeolian dune field. Overall, the dunes were probably a few metres high, and had simple, isolated, barchanoid or transverse forms based on the distribution of the grain-flow and grain-fall strata, the thickness of the grain-flow deposits, and their simple internal structure consisting in a single set of cross-strata with unimodal distribution of dip directions. The bounding surfaces at the bottom of the cross-stratified sandstone elements indicate that the dunes abutted on a concave-up excavation, 0.4 to 2 m deep, which is shaped like an elongated trough with a long axis approximately parallel to the foreset dip direction. This excavation can be attributed to the action of the airflow on the region of reattachment in front of the slip face. The thin interdune deposits (<0.3. m thick) that are rarely present at the base of the cross-stratified sets represent dry interdune deposits. The planar and erosional surfaces that define the top of the cross-stratified sets record deflation to the palaeo-water table (Stokes, 1968), as evidenced by (i) planar and wide extension in sections oriented both parallel and perpendicular to the direction of the foreset dip, (ii) small-scale erosional depressions and steps, which are considered to record erosion into cohesive damp sand (Kocurek, 1981; Kocurek and Day, 2018) and (iii) the type of overlying deposits, which accumulated on a damp surface.

Subcritical climbing translatent strata, granule ripples and adhesion ripples are the sedimentary structures that demonstrate an aeolian affinity for the planar-laminated sandstone and horizontally bedded sandstone elements (cf. Eriksson and Simpson, 1998). The surface microtextures of sand grains demonstrate aeolian transport. The tabular shape and large lateral continuity of these two elements demonstrates that they cannot be considered interdune deposits developed between coevally active migrating dunes arranged in a train (Kocurek, 1981). Nevertheless, these represent flat depositional areas, which can be generically termed sand sheets. The planar-laminated sandstone represents a dry sand sheet, the surface of which would have been covered by granule wind ripples and climbing wind ripples.

The horizontally bedded sandstone represents a damp sand sheet, the surface of which would have been covered by a microbial mat. Alternating episodes of deposition from high-energy winds and microbial colonisation contributed to the formation of biolaminites. The presence of microorganisms is suggested by the description of the MISS, the textural aspect of the sandstone, the taxonomic and biostratinomic aspects of the microfossil remains, and by chemical concentration of organic carbon (Wacey, 2009). Davies et al. (2016) questioned the interpretation of sedimentary structures named MISS as the product of biotic agents. Their criticism is based on the morphological similarity between present-day structures and MISS. These authors proposed a new descriptive classification that, in their opinion, can prevent misconceptions and misleading claims of MISS occurrences. MISS in the Venkatpur Sandstone Formation were recognised using an interdisciplinary (or holistic) approach, following that outlined by Noffke (2018) in her reply to Davies et al. (2016). Descriptions of morphological and textural features, comparison with abiotic structures, micropalaeontological taxonomic and biostratinomic aspects, and geochemical data (TOC and EDS) have been integrated to interpret the biotic origin of MISS (Noffke, 2009, 2010).

Occasional and localised floods formed temporary small and shallow lakes, where wind-generated waves reworked the recently wind-deposited sands. Decompacted vortex ripple height (see Supplementary material 1), ripple wavelength, vertical form index and grain size allow reconstruction of the ancient wave regime using the Airy linear wave theory. Estimation of the wave period (T) of the wave that originated the wave ripples and water depth were obtained using the method described by Immenhauser (2009). The calculated maximum wave period (T) is from 0.59 to 1.1 s and the water depth for the vortex ripple formation in Venkatpur Sandstone are 0.2-0.5 m for T=1.1 s and 0.04-0.5 m for T=0.59 s. See Supplementary material 2 for the calculation procedure. A wave period less than 4 s is considered typical of localised water masses with restricted fetch, for example as in small lakes, lagoons or ponds (Allen, 1984; Immenhauser, 2009).

5.2. Factors controlling aeolian-dominated systems with microbial mats

Overall, in the Venkatpur Sandstone Formation, the wind appears to be the main factor that governed sediment transport and deposition. In environments where the wind is the main agent of transport and deposition, two other factors, beyond the wind transport capacity, control the development of aeolian-dominated depositional environments: sediment supply and sediment availability (Kocurek and Lancaster, 1999; Kocurek, 2003).

The studied portion of the Venkatpur Sandstone Formation between Bellampalli and Mancherial is composed of a bulk of more than $1x10^{10}$ m^3 of sand. This demonstrates that this depositional system comprised a sufficient volume of sand to potentially construct a large erg system characterised by large-scale bedforms (Kocurek and Havholm, 1993; Kocurek, 1999).

Nevertheless, only small and simple dunes and aeolian sand sheets developed, probably because the availability of the sand for aeolian transport was markedly limited.

Facies analysis demonstrates that two important factors controlled the sand availability: water and the presence of biological agents capable of stabilising the landscape surface.

By acting to encourage adhesion of sand grains, water counteracts the erosive capacity of the wind and consequently decreases or eliminates the availability of sand for aeolian transport. In the Venkatpur Sandstone Formation, adhesion ripples, vortex ripples and MISS (biolaminites, petees, sand stromatolites, palimpsest ripples) testify the common occurrence of water at or above the accumulation surface of the horizontally bedded sandstone. Where did the water come from? The absence of evidence for fluvial or marine influence implies that that the presence of water was controlled exclusively by the water table, whose variations, probably a consequence of episodic rains and/or remote river-level oscillations and/or variations of the subsidence rate, could have influenced the nature of sedimentation.

The biological cover of the topographic surface was represented by microbial communities, which, by enveloping and covering the sand grains, bound and protected them from wind erosion and stabilised the sand surface (Eriksson et al., 2007; Gerdes, 2007). The stabilising influence of the microbial communities remained active when the water table dropped, because the dried microbial mat maintained its role as a stabilising agent on the ground surface. Thus, the presence of microbial mats constituted a more efficient means than the water table alone to restrict the availability of sand in this aeolian system.

The microbial communities associated with the horizontally bedded sandstone may be compared to present-day biological soil crusts (Belnap and Lange, 2001; Belnap, 2003; Weber et al., 2016). Biological soil crusts are microbial communities mainly composed of bacteria, bryophyte and lichens. They live within the first few millimetres of the soil surface in arid and semi-arid environments where the vascular plant cover is limited or absent. Biological soil crusts are important agents of pedogenesis and geomorphologic development in arid regions (Belnap, 2003; Williams et al., 2012). They fix C and N and capture dust nutrients, preparing the soil for vascular plants. They protect the soil from wind and water erosion. In the Chihauhan Desert, Belnap and Gillette (1998) observed that the threshold frictional velocity of the biological soil crusts (i.e. the force required to erode the soil particles) was well above the local wind forces; this characteristic was present year around, and also after long periods of drought. Biological soil crusts are strongly resistant to wind erosion and contribute to the stability of the soils (Belnap and Büdel, 2016). Thus, although very strong winds can break-up biological soil crusts (Amir et al., 2014), overall their presence decreases the availability of stored sand in aeolian-dominated systems. In Amargosa River flood plain, Ielpi (2019) suggested that biological soil crusts comprising halophytic microbial communities act to shelter the depositional surface by wind erosion, thereby contributing to channel stability. The microorganisms that currently compose biological soil crusts are similar to those that existed in Neoproterozoic time; hence it is reasonable to assume that they could have provided a similar function on the terrestrial surface (Belnap, 2003).

Depending on the sand availability, three different depositional settings are inferred. The first setting is represented by the cross-stratified sandstone, and is characterised by a field of simple and isolated dunes (Fig. 17A). The availability of sand was sufficient to construct the dunes, but not sufficient to generate compound or complex dunes, climbing dunes and thick intervening interdune deposits. External sand influx was insufficient to contribute to the construction of a system composed of large-scale aeolian bedforms and only small dunes developed; the shallow erosional surfaces below the cross-stratified sets suggest some internal reworking of sand via cannibalisation of underlying deposits. The second setting (planar-laminated sandstone) is characterised by a dry sand sheet (Fig. 17B), where the abundance of granule ripples testifies to undersaturated (i.e. locally deflationary) wind flows, as consequence of the restricted availability of sand for aeolian transport (Fryberger et al., 1979; Kocurek, 1981). The third setting (horizontally bedded sandstone) is represented by a damp sand sheet, where the growth of microbial communities and the deposition of biolaminites brought about a notable reduction in the availability of sand for aeolian transport (Fig. 17C). In this phase, the sedimentation was produced by occasional relatively high-energy wind flows, which deposited thin layers of medium- or fine-grained sand, followed by the action of microbial mats that baffled, trapped and bound fine- or very fine-grained sand grains transported by relatively low-energy wind flows.

The architectural elements that represent these three depositional settings alternate in the Venkatpur Sandstone Formation. The thickness of each of the accumulated elements is commonly less than 1 m , and apparently no erosional surfaces or palaeosols of regional extent divide them (Fig. 14). This implies that the transition from one setting to another was frequent and autogenic, rather than caused by drastic and externally forced environmental changes.

The occurrence of the three architectural elements can be depicted in an ideal sequence by a cartoon showing the succession of the depositional events and by a diagram representing the aeolian system sediment state (Kocurek and Lancaster, 1999; Kocurek, 1999) (Figs. 18 and 19). Isolated and simple dunes abutted on a flat surface previously colonised by microbial mats (Fig. 18A). An erosive airflow in front of the dunes dug a weak erosional surface 0.4 to 2 m deep. The flow conditions were sand saturated. A decrease in the sand supply and/or the progressive raise of the water table reduced the sand availability; the dunes ceased their migration and an erosional surface was cut to define the upper bounding surface of the accumulated cross-stratified set, with the level of erosion being limited by the capillary fringe of the water table. Microbial mats forming biolaminites developed atop the remnant dune accumulation (Fig. 18B). A renewed relative fall of the water table interrupted the microbial-mat growth, allowing the emplacement of aeolian granule ripples and sand wind ripples (Fig. 18C). A renewed increase in humidity favoured again the growth of microbial mats on the depositional surface (Fig. 18D).

Some clarifications are necessary before describing the sediment state of the aeolian system. For the simple model presented herein, the transport capacity of the wind and the duration of events are considered constant for each element; however, in fact, for units of a given thickness, the time of formation of cross-stratified sandstone and planar-laminated sandstone elements might have been longer than that of horizontally bedded sandstone. Most of the sediment supply was external, probably originating from the coastal environment that lay to the southeast, according to the provenance data of Joy et al. (2015) and the palaeoenvironmental reconstruction of Chakraborty (1991). Internal sediment supply was limited and derived from cannibalisation of previous deposits that were accumulated as cross-stratified sandstone, as suggested by the shallow and laterally restricted erosional surfaces at the bottom of this architectural element. The accumulation of the cross-stratified sandstone was characterised by higher influx of sediment: external with a subordinate contribution of internal supply (CLI in the terminology of Kocurek and Lancaster, 1999) (Fig. 19A). When this element was deposited, the sediment availability was at its maximum but still only marginally above the sediment influx because of the presence of lagged influx (CLI_{AL}); the transport capacity was above or coincident with available bulk of sediment, that is, the wind flows were saturated or almost saturated. The accumulation of the horizontally bedded sandstone coincided with a drastic reduction of the sediment availability, caused by the action of the microbial mats; the influx was exclusively external and probably less than that associated with emplacement of the other elements. The external influx was progressively stored below the microbial mats and the state of the aeolian system was characterised by CI_{AL} and S_{AL} fields (Fig. 19A). The planar-laminated sandstone was deposited in a regime of unsaturated wind flows, probably associated with a decrease of both sediment supply and sediment availability for aeolian transport. This represents intermediate conditions between the other two elements (CI_{AL}) (Fig. 19A) (cf. Kocurek and Nielson, 1981; Mountney and Russell, 2004).

Three mechanisms of accumulation are known for aeolian systems (Kocurek and Day, 2018): (i) in dry systems, the accumulation occurs due to climbing of dunes related to a decrease of wind transport capacity as a function of topography or in response to changing wind patterns; (ii) in wet systems it is related to rise of capillary fringe of the water table; (iii) in stabilising systems, the sand is accumulated in response to the stabilising influence of physical, chemical or biogenic factors, for example vegetation. A modified Wheeler diagram (Fig. 19B) aids in indicating the type and the rate of accumulation for the three architectural elements described above. The first element is characterised by simple and non-climbing dunes. Most of the sand deposited in this phase was eroded and the accumulated deposits comprise only small single-storey cross-stratified sets, truncated at their top by a planar erosional surface formed at the level of the capillary fringe of the water table. The second element is characterised by alternating phases of construction and erosion. The accumulation was probably controlled by the water table, because the overlying or interlayered strata were formed in damp conditions. The sediments of the third element do not record the generation of erosional surfaces, and their accumulation was associated with the stabilisation of the surface by microbial mats.

Although microbial mats are restricted to the horizontally bedded sandstone, the common and repeated alternation of this element with the others was crucial for the accumulation of the entire sedimentary succession. *De facto*, each time that the microbial mats covered the sandy accumulation surface, they protected the underlying accumulation from potential wind erosion, thus ensuring their long-term their accumulation.

6. CONCLUSIONS

In the Neoproterozoic Venkatpur Sandstone Formation, wind was the main agent of sediment transport and deposition. Associated with this, microbiological communities contributed directly and indirectly to the processes of sedimentation. This unit is composed of three architectural elements: cross-stratified sandstone, planar-laminated sandstone and horizontally bedded sandstone, which alternate within the sedimentary succession. These elements represent three depositional environments or settings: (i) fields of simple transverse or barchanoid dunes, (ii) dry sand sheet and (iii) damp sand sheet. Accumulation of the horizontally bedded sandstone element is interpreted to have been controlled by microbial mats, whose presence is suggested macroscopically by MISS (biolaminites, petees, sand stromatolites and palimpsest ripples) and microscopically by the morphology of the microfossils, which display concentrations of C, and by the occurrence of carbonaceous material in biolaminites.

This study attempted to answer three questions.

(i) Could the Precambrian microbial mats have contributed to the clastic depositional processes in an aeolian-dominated environment? The wind was the main agent of transport and sedimentation during emplacement of the cross-stratified sandstone and planar-laminated sandstone, whereas in the horizontally bedded sandstone the interaction of wind and microbial-mat growth formed biolaminites. Relatively high-energy wind deposited medium- or fine-grained sand, quickly colonised by microbial communities, which baffled, trapped and bound fine- or very fine-grained sand grains transported by low-energy winds. Thus, microbial mats, which may be compared with the present-day biological soil crusts, promoted the deposition of fine material and controlled the sand availability.

(ii) What was the large scale control of the microbial mats on construction and accumulation of the aeolian system? The depositional surfaces, which were covered by microbial mats, protected the underlining stored sediments from potential wind erosion. Microbial mats allowed the progressive and gradual vertical accumulation of sand by acting as an important stabilising agent that enabled long-term accumulation of the aeolian-dominated succession.

(iii) Were microbial mats a major reason why Precambrian aeolian successions tend to be simple in form and relatively uncommon? This question is for the moment without answer. The example of the Venkatpur Sandstone Formation cannot be extrapolated to all the Precambrian aeolian-dominated continental depositional systems, because the presence of microbial communities is not always evident and other environmental controlling factors can be more significant. However, this paper highlights that in Precambrian time, biotic communities likely exerted a greater influence on clastic sedimentation than has been considered hitherto.

ACKNOWLEDGEMENTS

The authors thank Prof. Dr. Tapan Chakraborty (GSU-ISI, India) for cooperation and prolific discussions during the field data collection. Dr. Erica Tonnetto, Josué Davi de Paula and Eufrásio José de Carvalho (State University of Campinas, Brazil) are acknowledged for technical help. Alessandro Ielpi and an anonymous reviewer provided helpful recommendations to improve this manuscript, as did Associate Editor Elson Paiva de Oliveira and Chief Editor Wilson Teixeira. This work was financed by FAPESP (Fundação de Amparo à Pesquisa do Estado de São Paulo) (project number 2017/03649-9) and CNPq (Conselho Nacional de Desenvolvimento Científico e Tecnológico) (project number 2018/3062762018-6).

REFERENCES

Abrantes Jr., F.R, Basilici, G. and Soares, T. M.V, 2020. Mesoproterozoic erg and sand sheet system: Architecture and controlling factors (Galho do Miguel Formation, SE Brazil). Precambrian Research, 338, https://doi.org/10.1016/j.precamres.2019.105592

Allen, J.R.L., 1979. A model for the interpretation of wave ripple-marks using their wavelength, textural composition, and shape. Journal of the Geological Society of London, 136, 673-682.

Allen, J.R.L., 1982. Sedimentary structures. Their character and Physical Basis, Vol. I. Elsevier, Amsterdam, 593 pp.

Allen, P.A., 1981. Some guidelines in reconstructing ancient sea conditions from wave ripplemarks. Marine Geology, 43, 59–67.

Allen, P.A., 1984. Reconstruction of ancient sea conditions with an example from the Swiss Molasse. Marine Geology, 60, 455–473.

Amir, R., Kinast, S., Tsoar, H., Yizhaq, H., Zaady, E. and Ashkenazy, Y., 2014. The effect of wind and precipitation on vegetation and biogenic crust covers in the Sde-Hallamish sand dunes, J. Geophys. Res. Earth Surf., 119, 437–450.

Astafieva, M. M., 2019. Archean Fossil Microorganisms. Paleontological Journal, 53, 228–240.

Bagnold, R.A., 1946. Motion of waves in shallow water: interactions between waves and sand bottom. Proc. Roy. Soc. London, 187, 1–15.

Basilici, G., Dal' Bó F.F.P., 2014. Influence of subaqueous processes on the construction and accumulation of an aeolian sand sheet. Earth Surface Processes and Landforms, 39, 1014–1029.

Battistuzzi, F.U., Feijao, A., Hedges, S.B., 2004. A genomic timescale of prokaryote evolution: insights into the origin of methanogenesis, phototrophy, and the colonization of land. BMC Evolutionary Biology, 4, 44-57.

Belnap, J., Lange, O.L. (Eds.), 2001. Biological Soil Crusts: Structure, Function, and Management. Ecological studies 150, Springer-Verlag, Berlin, Heidelberg, 503 pp.

Belnap, J., 2003. The World at Your Feet: Desert Biological Soil Crusts. Frontiers in Ecology and the Environment, 1, 181-189.

Belnap, J., Büdel, B., 2016. Biological Soil Crusts as Soil Stabilizers. In: Weber, B., Büdel, B., Belnap, J. (Eds.) Biological Soil Crusts: An Organizing Principle in Drylands. Ecological studies 226, Springer-Verlag, Berlin, Heidelberg, 304-320.

Belnap, J., Gillette D.A., 1998. Vulnerability of desert biological soil crusts to wind erosion: the influences of crust development, soil texture, and disturbance. Journal of Arid Environments, 39, 133–142.

Bottjer, D., Hagadorn, J.W., 2007. Mat Growth Features. In: Atlas of Microbial Mat Features Preserved within the Clastic Rock Record (Eds. J. Schieber, P.K. Bose, P.G. Eriksson, S. Banerjee, S. Sarkar, W. Altermann and O. Catuneanu), pp. 53-71. Elsevier, Amsterdam.

Bouougri, E. H., Porada, H., 2007. Mat-related features from the Neoproterozoic Tizi n-Taghatine Group, Anti-Atlas belt, Morocco. In: Atlas of Microbial Mat Features Preserved within the Clastic Rock Record (Eds. J. Schieber, P.K. Bose, P.G. Eriksson, S. Banerjee, S. Sarkar, W. Altermann, O. Catuneanu), pp. 198-207. Elsevier, Amsterdam.

Brookfield, M.E., 1977. The origin of bounding surfaces in ancient aeolian sandstones. Sedimentology, 24, 303-332.

Campbell, D.H., 1963. Percussion marks on quartz grains. J. Sediment. Petrol., 33, 855–859.

Chakraborty, T., 1991. Sedimentology of a Proterozoic erg: the Venkatpur Sandstone, P.G. Valley, South India. Sedimentology, 38, 301–322.

Chakraborty, T., Chaudhuri, A.K., 1993. Fluvial-aeolian interaction in a Proterozoic alluvial plain: example from the Mancheral Quartzite, Sullavi Group, Pranhita-Godavari Valley, India. In: The Dynamics and Environmental Context of Aeolianna Sedimentary Systems (Ed. K. Pye), Geol. Soc. Spec. Publ., 72, 127-141.

Chaudhuri, A.K., 1970. Precambrian stratigraphy and sedimentation around Ramgundam, Andhra Pradesh (unpubl. PhD Thesis). Calcutta University, 236 pp.

Chaudhuri, A.K., Deb, G.K., Patranabis-Deb, S., Sarkar, S., 2012. Paleogeographic and tectonic evolution of the Pranhita-Godavari valley, Central India: a stratigraphic perspective. American Journal of Science, 312, 766–815.

Collinson, J.C., Mountney, N.P., 2019. Sedimentary Structures. Dunedin Academic Press, Edinburgh, fourth edition, 340 pages. ISBN 978-1780460628.

Corbett, I.B., 2016. Sediment Dynamics of the Namib Aeolian Erosion Basin and the Arid Zone Diamond Placers of the Northern Sperrgebiet, Namibia. Memory of the Geological Survey of Namibia, 22, 6-171.

7Costa, P.J.M., Andrade, C., Mahaney, W.C., Marques da Silva, F., Freire, P., Freitas, M.C., Janardo, C., Oliviera, M.A., Silva, T., Lopes, V., 2013. Aeolian microtextures in silica spheres induced in a wind tunnel experiment: comparison with aeolian quartz. Geomorphology. 180–181, 120–129.

Davies, N.S., Gibling. M.R., 2012. Early Cambrian metazoans in fluvial environments, evidence of the non-marine Cambrian radiation: Comment. Geology, 40, 270.

Davies, N.S., Liu, A.G., Gibling, M.R., Miller, R.F., 2016. Resolving MISS conceptions and misconceptions: a geological approach to sedimentary surface textures generated by microbial and abiotic processes. Earth-Sci. Rev. 154, 210–246.

Eriksson, K.A., Simpson, E.L., 1998. Controls on spatial and temporal distribution of Precambrian eolianites. Sedimentary Geology, 120, 275–294.

Eriksson, P. G., Sarkar, S., Banerjee, S., Porada, H., Catuneanu, O., Samanta, P., 2010. Paleoenvironmental context of microbial mat related structures in siliciclastic rocks: Examples from the Proterozoic of India and South Africa. In: Microbial Mats: Modern and Ancient Microorganisms in Stratified Systems (Eds. J. Seckbach and A. Oren), pp. 73-108. Springer-Verlag, Berlin.

Eriksson, P.G., Catuneanu, O., Sarkar, S., Tirsgaard, H., 2005. Patterns of sedimentation in the Precambrian. Sedimentary Geology, 176, 17–42.

Eriksson, P.G., Schieber, P.G., Bouougri, E., Gerdes, G., Porada, H., Banerjee, S., Bose, P.K., Sarkar, S., 2007. Classification of Structures Left by Microbial Mats in Their Host Sediments. In: Atlas of Microbial Mat Features Preserved within the Clastic Rock Record (Eds. J.

Schieber, P.K. Bose, P.G. Eriksson, S. Banerjee, S. Sarkar, W. Altermann, O. Catuneanu), pp. 39-52. Elsevier, Amsterdam.

Eriksson, P.G., Simpson, E.L., Eriksson, K.A., Bumby, A.J., Steyn, G.L., Sarkar, S., 2000. Muddy roll-up structures in siliciclastic interdune beds of the ca. 1.8 Ga Waterberg Group, South Africa. Palaios, 15, 177–183.

Fryberger, S.G. and Schenk, C.J., 1988. Pin stripe lamination: a distinctive feature of modern and ancient eolian sediments. Sedimentary Geology, 55. 1-15.

Fryberger, S.G., Ahlbrandt, T.S., Andrews, S., 1979. Origin, sedimentary features, and significance of low-angle eolian 'sand sheet' deposits, Great Sand Dunes National Monument and vicinity, Colorado. Journal of Sedimentary Petrology, 49, 733-746.

Fryberger, S.G., Hesp, P. and Hastings, K., 1992. Aeolian granule ripple deposits, Namibia. Sedimentology, 39, 319–331.

Gavish, E., Krumbein, W.E., Halevy, J., 1985. Geomorphology mineralogy and groundwater geochemistry as factors of the hydrodynamic system of the Gavish Sabkha. In: Hypersaline Ecosystems - The Gavish Sabkha (Eds. G.M. Friedman, and W.E. Krumbein) Ecological Studies, 53, 186–217.

Gehling, J.G., 2000. Environmental interpretation and a sequence stratigraphic framework for the terminal Proterozoic Ediacara Member within the Rawnsley Quartzite, South Australia. Precambrian Research, 100, 65–95.

Gerdes, G., 2007. Structures left by modern microbial mats in their host sediments In: Atlas of Microbial Mat Features Preserved within the Clastic Rock Record (Eds. J. Schieber, P.K. Bose, P.G. Eriksson, S. Banerjee, S. Sarkar, W. Altermann and O. Catuneanu), pp. 5-38. Elsevier, Amsterdam.

Gerdes, G., Krumbein, W.E., 1987. Biolaminated Deposits, Berlin, Springer-Verlag, pp. 183

Gerdes, G., Klenke, T., Noffke, N., 2000. Microbial signatures in peritidal siliciclastic sediments: a catalogue. Sedimentology, 47, 279–308.

Gerdes, G., Krumbein, W.E., Reineck, H.E., 1991. Biolaminations—Ecological versus depositional dynamics. In: Cycles and Events in Stratigraphy (Eds. G. Einsele, W. Ricken, A. Seilacher) Springer-Verlag, Berlin, 592–607.

Gerdes, G., Krumbein, W.E., Reineck, H.E., 1994. Microbial mats as architects of sedimentary surface structures. In: Biostabilization of Sediments (Eds. W.E. Krumbein, D.M. Paterson, L.J. Stal), pp. 165–182. Bibliotheks und Informationssystem der Universität ldenburg, Oldenburg.

Goodall, T.M., North, C.P., Glennie, K.W., 2000. Surface and subsurface sedimentary structures produced by salt crusts. Sedimentology, 47, 99-118

Hunter, R.E., 1977a. Basic types of stratification in small eolian dunes. Sedimentology, 24, 361-387.

Hunter, R.E., 1977b. Terminology of cross-stratifi ed sedimentary layers and climbing-ripple structures basic types of stratification in small eolian dunes. Journal of Sedimentary Petrology, 47, 697-706.

Ielpi A., 2017. Lateral accretion of modern unvegetated rivers: remotely sensed fluvial–aeolian morphodynamics and perspectives on the Precambrian rock record. Geological Magazine, 154, 609–624.

Ielpi, A., 2018. River functioning prior to the rise of land plants: A uniformitarian outlook. Terra Nova, 30, 1–9.

Ielpi, A., 2019. Morphodynamics of meandering streams devoid of plant life: Amargosa River, Death Valley, California. GSA Bulletin, 131, 782–802.

Ielpi, A., Ghinassi, M., Rainbird, R.H., Ventra, D., 2018. Planform sinuosity of Proterozoic rivers: A craton to channel-reach perspective. In: Ghinassi, M., Colombera, L., Mountney, N.P.

and Reesink, A.J. (Eds.), Fluvial Meanders and their Sedimentary Products in the Rock Record. International Association of Sedimentologists Special Publication, 48, 81 –118.

Immenhauser, A., 2009. Estimating palaeo-water depth from the physical rock record. Earth-Science Reviews, 96, 107–139.

Joy, S., Jelsma, H., Tappe, S., Armstrong, R., 2015. SHRIMP U–Pb zircon provenance of the Sullavai Group of Pranhita–Godavari Basin and Bairenkonda Quartzite of Cuddapah Basin, with implications for the Southern Indian Proterozoic tectonic architecture. Journal of Asian Earth Sciences, 111, 827–839.

Kocurek, G., 1981. Significance of interdune deposits and bounding surfaces in aeolian dune sands. Sedimentology, 28, 753–780.

Kocurek, G., 1999. The Aeolian rock record (Yes, Virginia, it exists, but it really is rather special to create one). In: Aeolian Environments, Sediments and Landforms (Eds. A.S. Goudie, I. Livingstone), pp. 239-259. John Wiley and Sons, Chichester.

Kocurek, G., 2003. Limits on extreme eolian systems: Sahara of Mauritania and Jurassic Navajo Sandstone examples. In: Extreme Depositional Environments: Mega end Members in Geological Time (Eds. M.A. Chan, A.W. Archer), Geological Society of America Special Paper, 370, 43–52.

Kocurek G., Nielson J., 1986. Conditions favourable to the formation of warm-climate aeolian sand sheets. Sedimentology, 33, 795–816.

Kocurek, G., Day, M., 2018. What is preserved in the aeolian rock record? A Jurassic Entrada Sandstone case study at the Utah–Arizona border. Sedimentology, 65, 1301–1321.

Kocurek, G., Dott, R.H., 1981. Distinctions and uses of stratification types in the interpretation of eolian sand. Journal of Sedimentary Petrology, 51, 579–595.

Kocurek, G., Fielder, G., 1982. Adhesion structures. Journal od Sedimentary Petrology, 52, 1229-1241.

Kocurek, G., Havholm KG., 1993. Aeolian sequence stratigraphy - a conceptual framework. In: Siliciclastic Sequence Stratigraphy. Recent Developments and Applications (Eds. P. Weimer, H. Posamentier). American Association of Petroleum Geologists, Memoir 58, 393–409.

Kocurek, G., Lancaster, N., 1999. Aeolian system sediment state: theory and Mojave Desert Kelso dune field example. Sedimentology, 46, 505–515.

Kocurek, G., Nielson, J., 1986. Conditions favourable to the formation of warm-climate aeolian sand sheets. Sedimentology, 33, 795–816.

Krinsley, D.H., Donahue, J., 1968. Environmental interpretation of sand grain surface textures by electron microscopy. Geol. Soc. Am. Bull., 79, 743–748.

Krinsley, D.H., Friend, P.F., Klimentidis, R., 1976. Eolian transport textures on the surfaces of sand grains of Early Triassic age. Geol. Soc. Am. Bull., 87, 130–132.

Krinsley, D.H., Trusty, P., 1985. Environmental interpretation of quartz grain surface textures. In: Suffer, G.G. (Ed) Provenance of Arenites, 213–229. Dordrecht: Reidel.

Lancaster, N., 1995. Geomorphology of desert dunes. Routledge Physical Environment Series, London and New York, 244 pp.

Lancaster, N., Baas, A., 1998. Influence of vegetation cover on sand transport by wind: field studies at Owens Lake, California. Earth Surface Processes and Landforms, 23, 69-82.

Li, Q., Chen, X., Jiang, Y., Jiang, C., 2016. Morphological Identification of Actinobacteria. In: Dhanasekaran, D., Jiang, Y. (Eds) Actinobacteria - Basics and Biotechnological Applications. InTech, Rijeka, pp. 59−86

Long, D.G.F., 2006. Architecture of pre-vegetation sandy-braided perennial and ephemeral river deposits in the Paleoproterozoic Athabasca Group, northern Saskatchewan, Canada as indicators of Precambrian fluvial style. Sedimentary Geology, 190, 71–95.

Mahaney,W.C., 2002. Atlas of Sand Grain Surface Textures and Applications. Oxford University Press, Oxford, 237 pp.

Margolis, S.V., Krinsley, D.H., 1971. Submicroscopic frosting on Eolian and subaqueous quartz sand grains. Geol. Soc. Am. Bull. 82, 3395–3406.

Margolis, S.V., Krinsley, D.H., 1974. Processes of formation and environmental occurrence of microfeatures on detrital quartz grains. Am. J. Sci., 274, 449–464.

McCowen, J., 1894. On the highest wave of permanent type. Philos. Mag., 5, 351--357.

McKee, E. D. (1966) Structures of dunes at White Sands National Monument, New Mexico. Sedimentology, 7, 3–69.

Miche, R., 1944. Undulatory movements of the sea in constant and decreasing depth. Annu. de Ponts et Chaussées, May-June, July-August, pp. 25-75, 131-164, 270-292, 369-406.

Miller, M.C., Komar, P.D., 1980. Oscillation sand ripples generated by laboratory apparatus. Journal of Sedimentary Petrology, 50, 173–182.

Mountney, N.P., Russell, A. J., 2004. Sedimentology of cold-climate aeolian sandsheet deposits in the Askja region of northeast Iceland. Sedimentary Geology, 166, 223–244.

Mountney, N.P., Russell, A. J., 2006. Coastal aeolian dune development, Sólheimasandur, southern Iceland. Sedimentary Geology, 192, 167–181.

Mountney, N.P., Russell, A. J., 2009. Aeolian dune-field development in a water table-controlled system: Skeiđdarársandur, Southern Iceland. Sedimentology, 56, 2107–2131.

Mountney, N.P., Thompson, D.B., 2002. Stratigraphic evolution and preservation of aeolian dune and damp/wet interdune strata: an example from the Triassic Helsby Sandstone Formation, Cheshire Basin, UK. Sedimentology, 49, 805–833.

Noffke, 2009. The criteria for the biogeneicity of microbially induced sedimentary structures (MISS) in Archean and younger, sandy deposits. Earth-Science Reviews, 96, 173–180.

Noffke, N., 2010. Microbial mats in sandy deposits. Elsevier, Amsterdam, 196 pp.

Noffke, N., 2018. Comment on the paper by Davies et al. “Resolving MISS conceptions and misconceptions: A geological approach to sedimentary surface textures generated by microbial and abiotic processes” (Earth Science Reviews, 154 (2016), 210–246). Earth-Science Reviews,176, 373–383.

Noffke, N., Gerdes, G., Klenke, T., Krumbein, W. E., 2001. Microbially induced sedimentary structures - a new category within the classification of primary sedimentary structures. Journal of Sedimentary Research, 71, 649–656.

Noffke, N., Gerdes, G., Klenke, T., Krumbein, W.E., 1997. A microscopic sedimentary succession of graded sand and microbial mats in modem siliciclastic tidal flats. Sedimentary Geology, 110, 1-6.

Pye, K., Tsoar, H., 2009. Aeolian Sand and Sand Dunes. Springer-Verlag, Berlin Heidelberg, 458 pp.

Qian, G., Dong, Z., Zhang, Z., Luo, W., Lu, J., 2012. Granule ripples in the Kumtagh Desert, China: Morphology, grain size and influencing factors. Sedimentology, 59, 1-14.

Reineck, H.E., 1955. Hattripplen und haftwarzen, Ablagerungs Formenvon Flugsand. Senckenbergiana Lethaea, 36, 347-357.

Reineck, H.E., Gerdes, G., Claes, M., Dunajtschik, K., Riege, H., Krumbein, W.E., 1990. Microbial modification of sedi-mentary structures. In: Sediments and Environmental Geochemistry (Eds. D. Helrig, P. Rothe, U. Förstner, P. Stoffers), pp. 254–276. Springer, Berlin.

Retallack, G.J., 2001. Soils of the Past: An Introduction to Paleopedology 2nd edn., Blackwell, Oxford, 404 pp.

Retallack, G.J., 2014. Precambrian life on land. The Palaeobotanist, 63, 1–15.

Retallack, G.J., Krinsley, D.H., Fischer, R., Razink, J.J., Langworthy, K.A., 2016. Archean coastal-plain paleosols and life on land. Gondwana Research, 40, 1-20.

Rodríguez-López, J.P. Clemmensen, L.B., Lancaster, N., Mountney, N.P., Veiga, G.D., 2014. Archean to Recent aeolian sand systems and their sedimentary record: current understanding and future prospects. Sedimentology, 61, 1487–1534.

Romain, H., Mountney, N.P., 2014. Reconstruction of three-dimensional eolian dune architecture from one-dimensional core data through adoption of analog data from outcrop. American Association of Petroleum Geologists Bulletin, 98, 1-22.

Rubin, D.M., 1987. Cross-bedding, bedforms and palaeocurrents. SEPM Concepts Sedimentol. Paleontol., 1, 187 p.

Rubin, D.M., Carter, C.L., 2006. Cross-bedding, bedforms, and paleocurrents. SEPM Concepts Sedimentol. Paleontol., 1, 2nd edn, 195 p.

Santos, M.G.M., Mountney, N.P., Peakall, J., 2016. Tectonic and environmental controls on Palaeozoic fluvial environments: reassessing the impacts of early land plants on sedimentation, Journal of the Geological Society, 174, 393-404.

Schidlowski, M.A., 2005. Paleobiological and biogeochemical vestiges of early terrestrial biota: baseline for evaluation of extraterrestrial evidence. (In: R.B. Hoover et al., Perspectives in Astrobiology), IOS Press, Amsterdam, Berlin, Oxford, Tokyo, Washington, 146–169.

Schieber, J., 2004. Microbial Mats in the Siliciclastic Rock Record: A Summary of Diagnostic Features. In: The Precambrian Earth: tempos and events (Eds. P.G. Eriksson, W. Altermann, D.R. Nelson, W.U. Mueller, O. Catuneaunu). Developments in Precambrian Geology, 12, 663-672.

Sharp, R.P., 1963. Wind Ripples. The Journal of Geology, 71, 617-636

Sheldon, N.D., Retallack, G.J., 2001. Equation for compaction of palaeosols due to burial. Geology, 29, 247–250.

Simpson, E.L., Alkmim, F.F., Bose, P., Bumby, A., Eriksson, P.G., Eriksson, K.A., Martins-Neto, M., Middleton L., Rainbird, R., 2004. Sedimentary Dynamics of Precambrian Aeolianites. In: The Precambrian Earth: tempos and events (Eds. P.G. Eriksson, W. Altermann, D.R. Nelson, W.U. Mueller, O. Catuneaunu). Developments in Precambrian Geology, 12, 642–657.

Simpson, E.L., Heness, E., Bumby, A., Eriksson, P.G., Eriksson, K.A., Hilbert-Wolf, H.L., Linnevelt, S. Malenda, H.F., Modungwa, T., Okafor, O.J., 2013. Evidence for 2.0 Ga continental microbial mats in a paleodesert setting. Precambrian Research, 237, 36–50.

Smoot, J.P., Castens-Seidell, B., 1994. Sedimentary features produced by efflorescent crusts, Saline Valley and Death Valley, California. In: Renaut, R.W., Last, W.M. (Eds) Sedimentology and Geochemistry of Modern Ancient Saline Lakes. Spec. Publ. Soc. Econ. Paleont. Miner., Tulsa, 50, 73-90.

Stokes, W.L., 1968. Multiple parallel-truncation bedding planes—a feature of wind-deposited sandstone. Journal of Sedimentary Petrology, 55, 361–365.

Vos, K., Vandenberghe, N., Elsen, J., 2014. Surface textural analysis of quartz grains by scanning electron microscopy (SEM): from sample preparation to environmental interpretation. Earth Sci. Rev. 128, 93–104.

Wacey, D., 2009. Early life on earth: a practical guide, Springer, 274 pp.

Watanabe, Y., Martini, J.E.J., Ohmoto, H., 2000. Geochemical evidence for terrestrial ecosystems 2.6 billion years ago. Nature, 408, 574–578.

Weber, B., Büdel, B., Belnap, J., (Eds.) (2016) Biological Soil Crusts: An Organizing Principle in Drylands. Ecological studies 226, Springer-Verlag, Berlin, Heidelberg, 549 pp.

Westall, F., 2005. Life on the early Earth: a sedimentary view. Science, 308, 366-367.

Westall, F., Steele, A., Toporski, J., Walsh, M., Allen, C., Guidry, S., Gibson, E., Mckay, D., Chafetz, H., 2000. Polymeric substances and biofilms as biomarkers in terrestrial materials: Implications for extraterrestrial samples. Journal of Geophysical Research, 105, 24,511–24,527,

Westall, F., de Vries, S.T., Nijman, W., Rouchon, V., Orberger, B., Pearson, V., Watson, J., Verchovsky, A., Wright, I., Rouzaud, J.-N., Marchesini, D., Severine, A., 2006. The 3.466 Ga “Kitty’s Gap Chert,” an early Archean microbial ecosystem. In Reimold, W.U., Gibson, R.L. (Eds) Processes on the Early Earth. Geological Society of America Special Paper 405, 105–131.

Williams, A.J., Buck, B.J., Beyene, M.A., 2012. Biological Soil Crusts in the Mojave Desert, USA: Micromorphology and Pedogenesis. Soil Science Society of America J., 76, 1685-1695.

CAPTIONS

Figure 1. Geographical and geological map of study area and neighbouring. Modified by Chakraborty and Chaudhuri (1993).

Figure 2. Cross-stratified sandstone architectural element. (A) Small lenses of coarse-grained sandstone are more common in upper portion of the cross stratifications. They can display weakly erosive bottom (arrow). These lenses are interpreted as grain-flow deposits. The subdivisions of the Jacob's staff are 0.1 m. (B) Medium-grained sandstone foresets are typical of the upper portion of the cross stratification. Sometimes they show weak inverse grading (arrow). Few fine-grained sandstone foreset laminae are alternated to medium-grained sandstone foresets. Medium-grained sandstone foresets are interpreted as grain-flow deposits. Coin: 22 mm in diameter. (C) Medium-grained sandstone laminae are localised even in tangential bottom portion of the cross stratifications (arrows); they are interpreted as wind ripples deposits. The subdivisions of the Jacob's staff are 0.1 m. (F) Fine-grained sandstone foresets are common on the middle and lower portion of the cross stratifications. They can be interpreted as grain-fall deposits. Coin: 22 mm in diameter. (E) Cross-stratified sandstone. The top surface of this set is erosive and characterised by small steps corresponding to the cross stratifications. These aspects are attributed to erosion in cohesive damp sand.

Figure 3. Cross-stratified sandstone architectural element. The cross stratification sets alternate with horizontally bedded sandstone element. The exposure is parallel to the dip of the

cross-strata. The arrow indicates an upwind termination of a cross stratification set; note the erosive bottom. This succession corresponds to interval 9 to 15 m of Figure 14A.

Figure 4. The tangential bottom foresets of cross-stratified sandstone occasionally climb on their horizontal terminations. In this case, the line which joins the points where the inclined foresets approach to the horizontal (dotted in this picture) is an inclined (up to 7°) climbing surface. The cross stratification overlies horizontally bedded sandstone element. The subdivisions of the Jacob's staff are 0.1 m.

Figure 5. The three architectural elements are alternated in section parallel to the dip direction of the cross-strata. Note the planar, continuous and parallel bounding surfaces of the all the three elements and their long lateral continuity without significant thickness variations. Small and lenticular cross-stratified sets are enclosed by horizontally bedded sandstone or planar-laminated sandstone; they represent small dunes in sand sheet environment. Site located c. 8 km to NNW of Mancherial.

Figure 6. Section perpendicular to the dip direction of the cross-strata. In this section, the bottom bounding surfaces of the cross stratification is clearly concave up, cutting the underlying horizontally bedded sandstone or planar laminations sandstone. The intersection of this section with the section parallel to the cross-strata demonstrates that the cross-strata abut on an elongated erosive trough. Site located c. 8 km to NNW of Mancherial.

Figure 7. Dip directions of the cross stratifications of cross-stratified sandstone architectural element. These uniform values suggest that the cross-strata were formed by straight-crested transverse or barchanoid dunes.

Fig. 8. Planar-laminated sandstone architectural element. (A) Thin layers comprising alternating planar laminae of fine- to medium-grained sandstone pass gradually upward to medium- to coarse-grained sandstone. Note the lenticular coarse-grained layers with convex up top (arrows), where coarse grains are concentrated in some cases. These sedimentary structures are interpreted as small granule ripples (Fryberger et al., 1992). Coin: 23 mm in diameter. (B) Small lens of low-angle, fine- to coarse-grained sandstone foresets alternating with planar layers described in (A). These cross-stratified small lenses correspond to large granule ripples of Fryberger et al. (1992). Coin: 25 mm in diameter. (C) Fine- to medium-grained thin continuous laminae, some with weak inverse grading. These deposits are interpreted as subcritical climbing translatent strata. They alternate with granule-ripple deposits as in the lower portion of the picture. Coin: 23 mm in diameter.

Figure 9. Lithofacies of the horizontal bedding sandstone architectural element. (A) Typical dichromatic aspect of the principal lithofacies of this architectural element: planar (i) or irregular (ii) horizontal bedding. The upper portion of the photo depicts cross stratification with an undulating erosional top surface interpreted as recording erosion to the capillary fringe of the palaeo-water table. (B) Microphotograph of a thin layer of medium-grained sandstone (a) passing upward to fine-grained layers (b). Note the sharp bottom and the reddish-brown concentration of oxides and hydroxides on the fine-grained layer and on the top. This layers correspond to the microsequences described by Noffke et al. (1997) and Noffke (2010) and are interpreted as biolaminites. (C) Larger layers of the planar or irregular horizontal beds are characterised by medium-grained sandstone with planar laminations, similar to pin stripe laminations, and small-scale cross lamination (indicated by the arrow). These structures are interpreted as having been deposited by wind ripples. The coin of 5 rupees is 23 mm in diameter. (D) Fine-grained portion of

thin layers of planar or irregular horizontal beddings showing grains with long-axes orientated parallel to the stratification (arrows). This suggests that they assumed this suitable position to the gravity by the reduction of the friction for the presence of soft organic matter (cf. Noffke et al., 1997). Note the concentration of oxides and hydroxides in this upper portion of the layers. (E) The irregular horizontal beddings are similar to the planar horizontal bedding, but the former is characterised by layers that are undulating or contorted, forming small domes or narrow anticlines. In general the height of these structures is less than 20 mm, but in some cases, as shown in this picture, it can be larger than 50 mm. Coin: 23 mm in diameter.

Figure 10. (A) Frequency distribution of the surface microtextures of sand grains in coarser layer of planar or irregular horizontal bedding lithofacies of the horizontally bedded sandstone element. The described features are typical of an aeolian-dominated depositional setting. (B) Almost all the grains exhibit a rounded outline and, low relief (a smooth surface that lacks significant local irregularity); bulbous edges and elongated or equidimensional depressions are common. (C) Upturned plates, which are present in 80% of the sand grains, are characteristic of aeolian transport (Margolis and Krinsley, 1971). (D) Crescentic percussion marks are curved fractures formed by grain-to-grain collisions in aeolian environments (Campbell, 1963).

Figure 11. Lithofacies of the horizontally bedded sandstone architectural element. (A) Small domes in irregular horizontal beddings lithofacies. The domes are composed of laminae of fine-grained sandstone and the nucleus is constituted of structureless medium-grained sandstone (see yellow arrows). At the margins of the domes, thin alternating laminae of fine- and medium-grained sandstone onlap the upturned margins of the domes (see black arrow). These structures are interpreted as petee, a MISS produced by deformation of the microbial mat surface by upwelling of underlying gases produced by the decay of organic matter. (B) Some domes show a

ruptured crest, probably generated when the elevated gas pressure broke the microbial mat crust. Coin: 23 mm in diameter. (C) Small flattened domes of sandstone are commonly visible on the bed surface of fine-grained laminae. They are attributed to a type of MISS, named sand stromatolite. Alternatively, they may correspond to microbial communities grown on small mat chips. (D) In some cases, the domes described in (C) cover the crest of wave ripples (arrow). (E) Small planar-concave lenses of medium-grained sandstone (arrows), aligned along the bed surface, are relatively common in the horizontal bedding sandstone. Coin: 23 mm in diameter. (F) On bed surfaces it is possible observe that the same small planar-concave lens of medium-grained sandstone, observed in picture E, corresponds to the upcurrent portion of adhesion ripples (arrow). Coin: 20 mm.

Figure 12. Lithofacies of the horizontally bedded sandstone architectural element. (A) Set with irregular cross-stratification attributable to climbing adhesion ripples. Coin: 23 mm in diameter. (B) Symmetrical vortex ripples formed in small and temporary ponds. Coin: 23 mm in diameter. (C) Climbing vortex ripples, which indicate wave action in conditions of high rates of sediment input. Coin: 23 mm in diameter. (D) Two overlapping generations of analogous vortex ripples. The non-destructive relationship with the previous ripple forms is attributed to the stabilising action of the microbial mat. This type of MISS is named palimpsest ripples. Coin: 23 mm in diameter.

Figure 13. Cartoon showing the formation of biolaminites in an aeolian-dominated environment. (A) The wind, probably a sand storm, deposits a thin layer of medium- or fine-grained sand. In thicker layers pin-stripe laminations and small wind-generated cross laminations are visible. (B) Microbial communities begin to grow on the surface of the sand, producing a microbial mat. (C) Microbial mat growths and fine- or very fine-grained sand grains are baffled,

trapped and bound by the adhesive properties of bacteria and extracellular polymeric substance (EPS).

Figure 14. (A) Typical sections of Venkatpur Sandstone Formation. (A) Site of Gurvapur, c. 11 km from Bellampalli toward SW. (B and C) Site of Gaandhaari Maisamma Temple, c. 8 km from Mancherial toward the NNW. Elements of horizontally bedded sandstone, which constitutes most of the succession, alternate vertically with element of cross-stratified sandstone and planar-laminated sandstone.

Figure 15. Microfossil from the fine- or very fine-grained laminae of horizontally bedded sandstone. (A) Filamentous structures, which may be interpreted as bacteria with spiral form (Spirillum). The arrow shows thin striae lengthwise. (B) Carbon EDX (electron diffraction X-ray spectrometry) map of the microfossil of figure (A). (C) EDX spot analysis of the filamentous microfossil made at the yellow spot in figure (A). The peak of the carbon is small relative to the other elements because the electron beam of the SEM is larger than the dimension of the microfossil. (D) A colony of coccoid bacteria microfossils indicated by the arrows. (E) Coccoid bacteria with wrinkle surface indicating post mortem fossilisation. The coating grain surface around the coccoid form probably corresponds to EPS (extracellular polymeric substance). (F) Carbon EDX (electron diffraction X-ray spectrometry) map of the microfossil of figure (E).

Figure 16. Microfossil from the fine- or very fine-grained laminae of the horizontally bedded sandstone. (A) EDX spot analysis of the coccoid microfossil made at yellow spot of figure 15E. (B) Rod bacteria microfossil (arrow) coated and enveloped by EPS. Note the two rod cells separated by a "neck", that indicate a phase of cell division. (C) Sheath bacteria microfossils are tubular forms with wrinkly superficial texture, in some cases deformed and squashed as here. (D)

EPS envelops and covers various microfossils (coccoids, rods and sheaths), indicated by the arrows. The alveolar structure of EDS is indicated with circles.

Figure 17. Graphic representation of three depositional environments as represented by the deposits of three architectural elements in the Venkatpur Sandstone Formation. See text for discussion.

Figure 18 Cartoon showing a model of events that led to the construction and accumulation of the Venkatpur Sandstone Formation. See text for discussion.

Figure 19. (A) Sediment state diagram of the aeolian-dominated system of Venkatpur Sandstone Formation. See text for discussion. For architectural elements: 1 = cross-stratified sandstone; 2 = planar parallel sandstone; 3 = horizontally bedded sandstone. CLI_{AL}: contemporaneous and lagged influx, availability limited; CI_{AL}: contemporaneous influx, availability limited; S_{AL}: stored availability limited.

Table 1. Petrographic mean composition of 11 samples of fine- and medium-grained sandstone of the three architectural elements. Overall, the sandstone can be classified as sublitharenite.

Table 2. Summary of architectural elements and lithofacies observed in the Venkatpur Sandstone Formation.

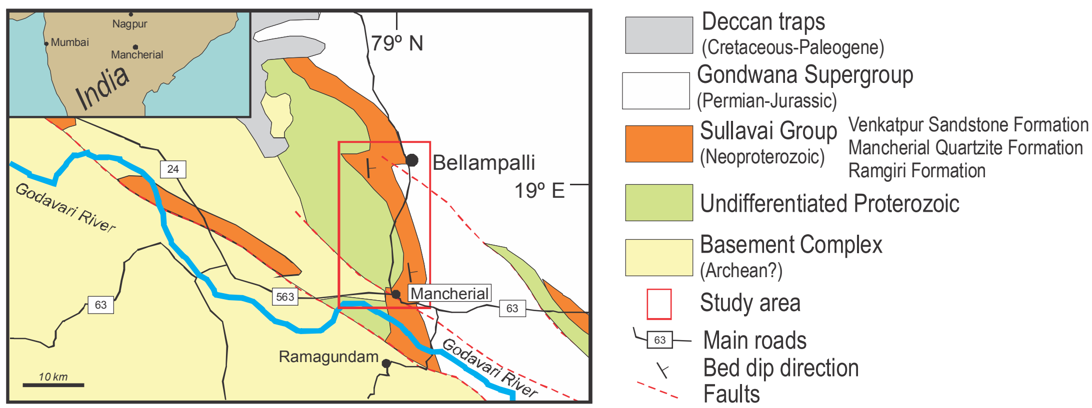

Nagpur
Mumbai
Mancherial
India
79º N
Bellampalli
19º E
24
Godavari River
563
Mancherial
63
63
Ramagundam
Godavari River
10 km
Deccan traps
(Cretaceous-Paleogene)
Gondwana Supergroup
(Permian-Jurassic)
Sullavai Group
(Neoproterozoic)
Venkatpur Sandstone Formation
Mancherial Quartzite Formation
Ramgiri Formation
Undifferentiated Proterozoic
Basement Complex
(Archean?)
Study area
Main roads
Bed dip direction
Faults

FIGURE 1

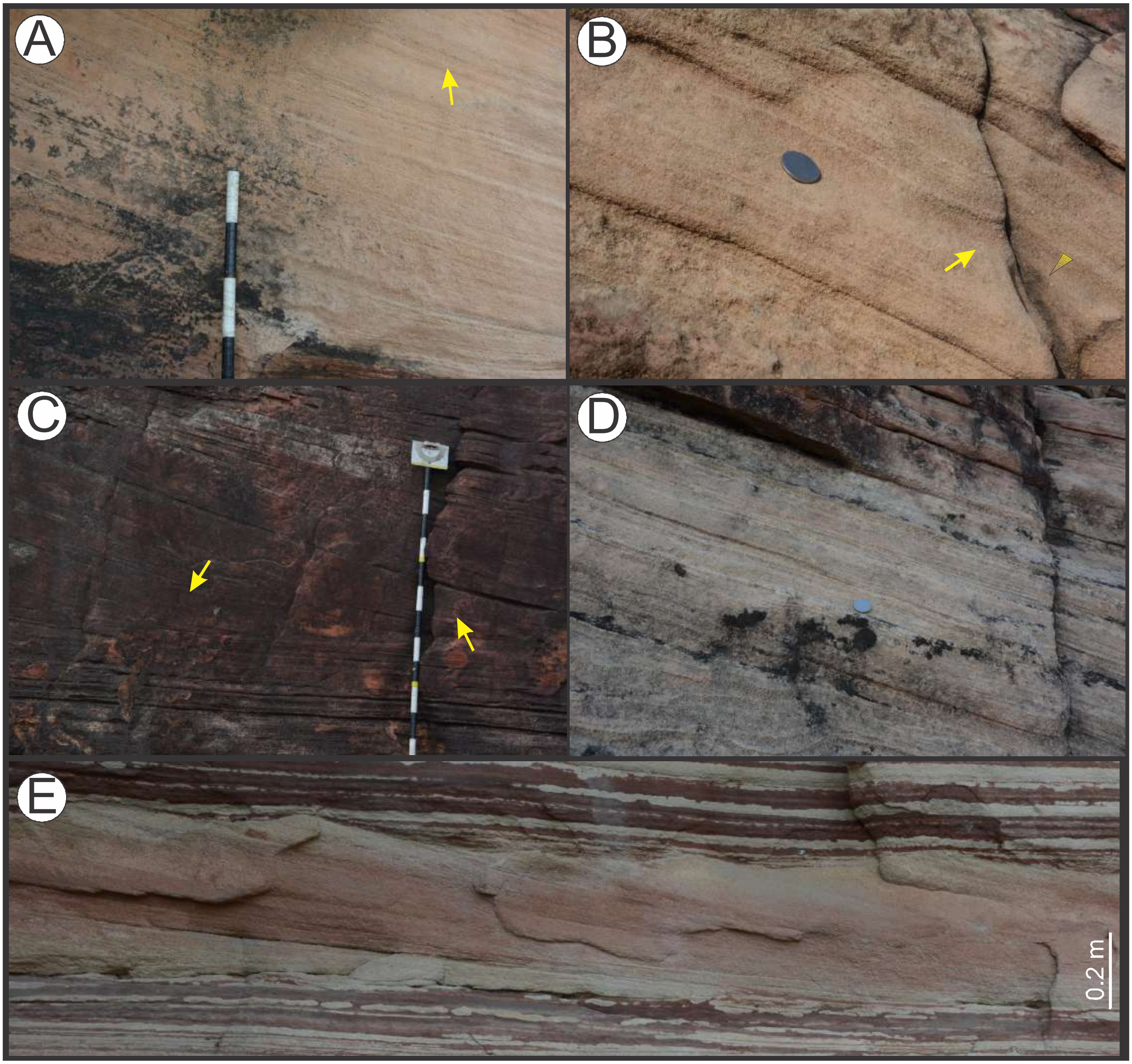

FIGURE 2

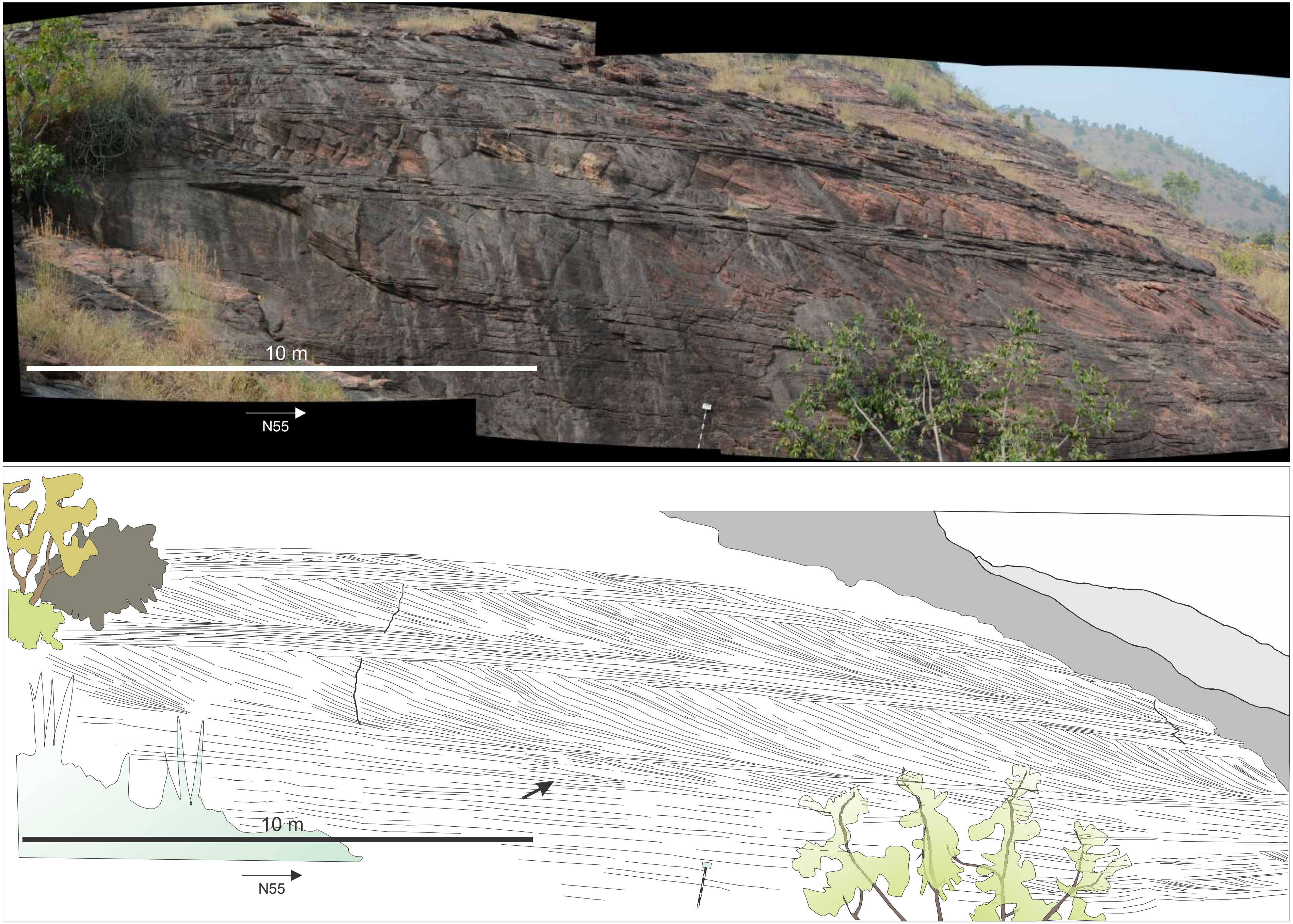

FIGURE 3

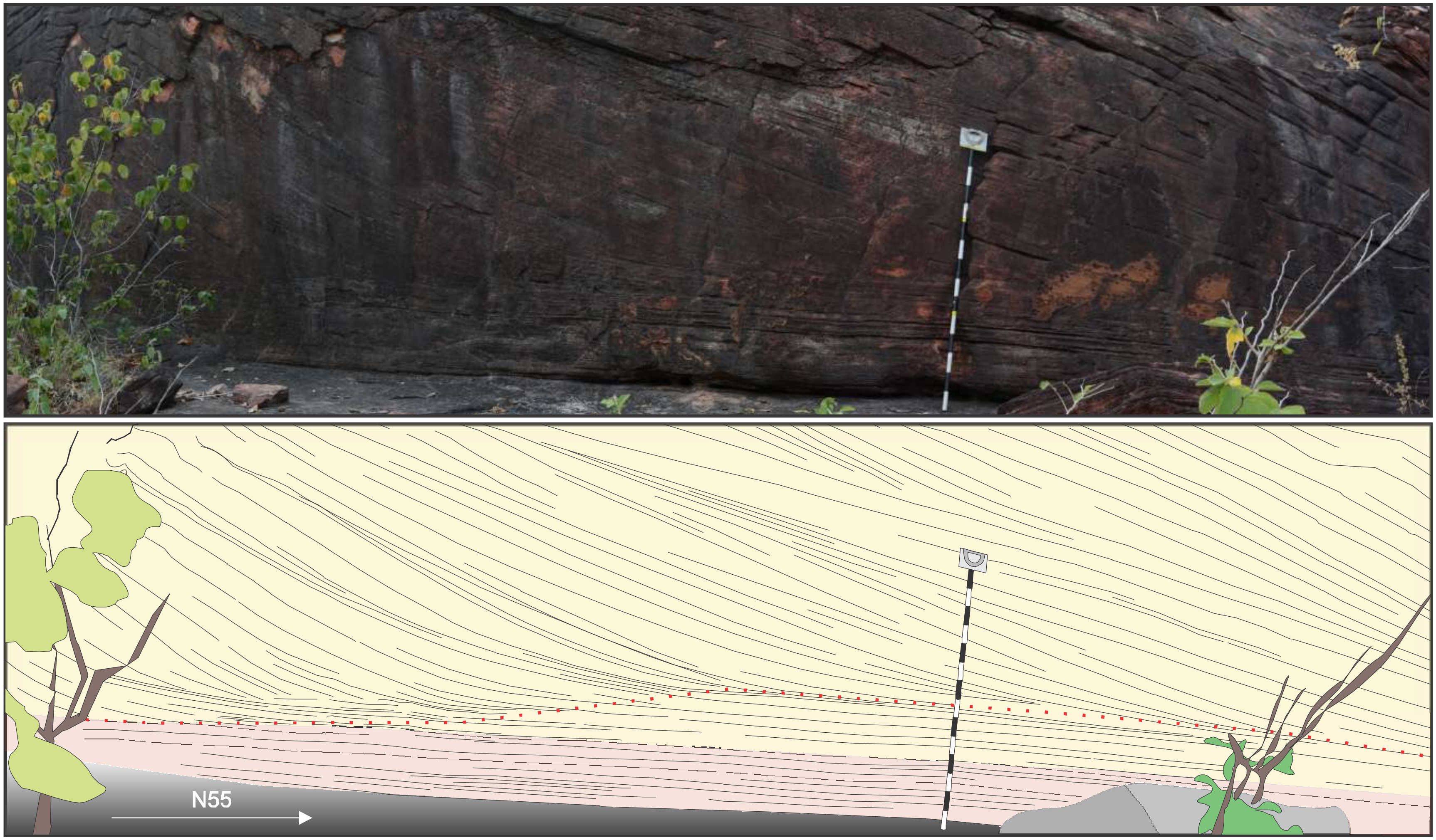

FIGURE 4

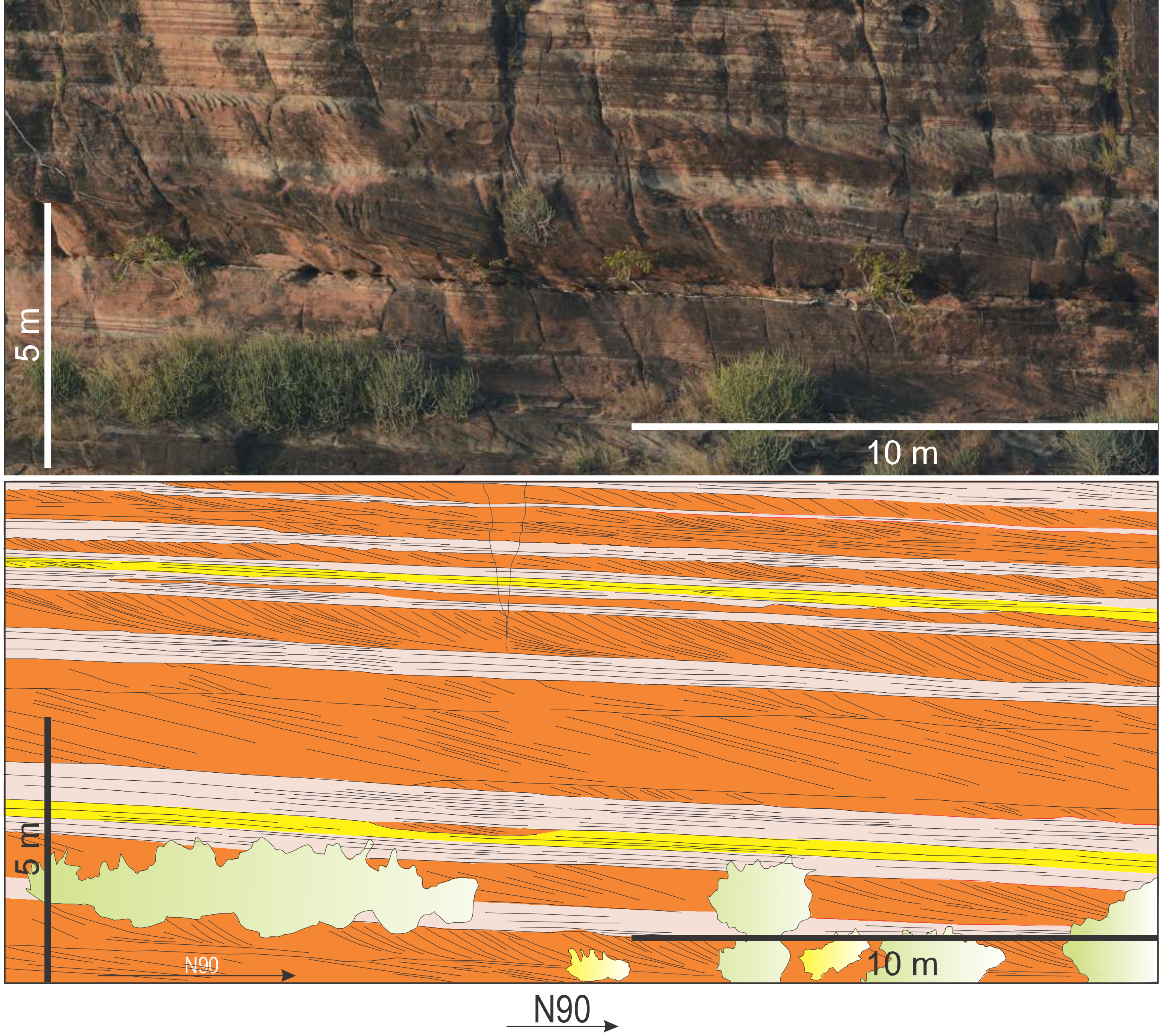

FIGURE 5

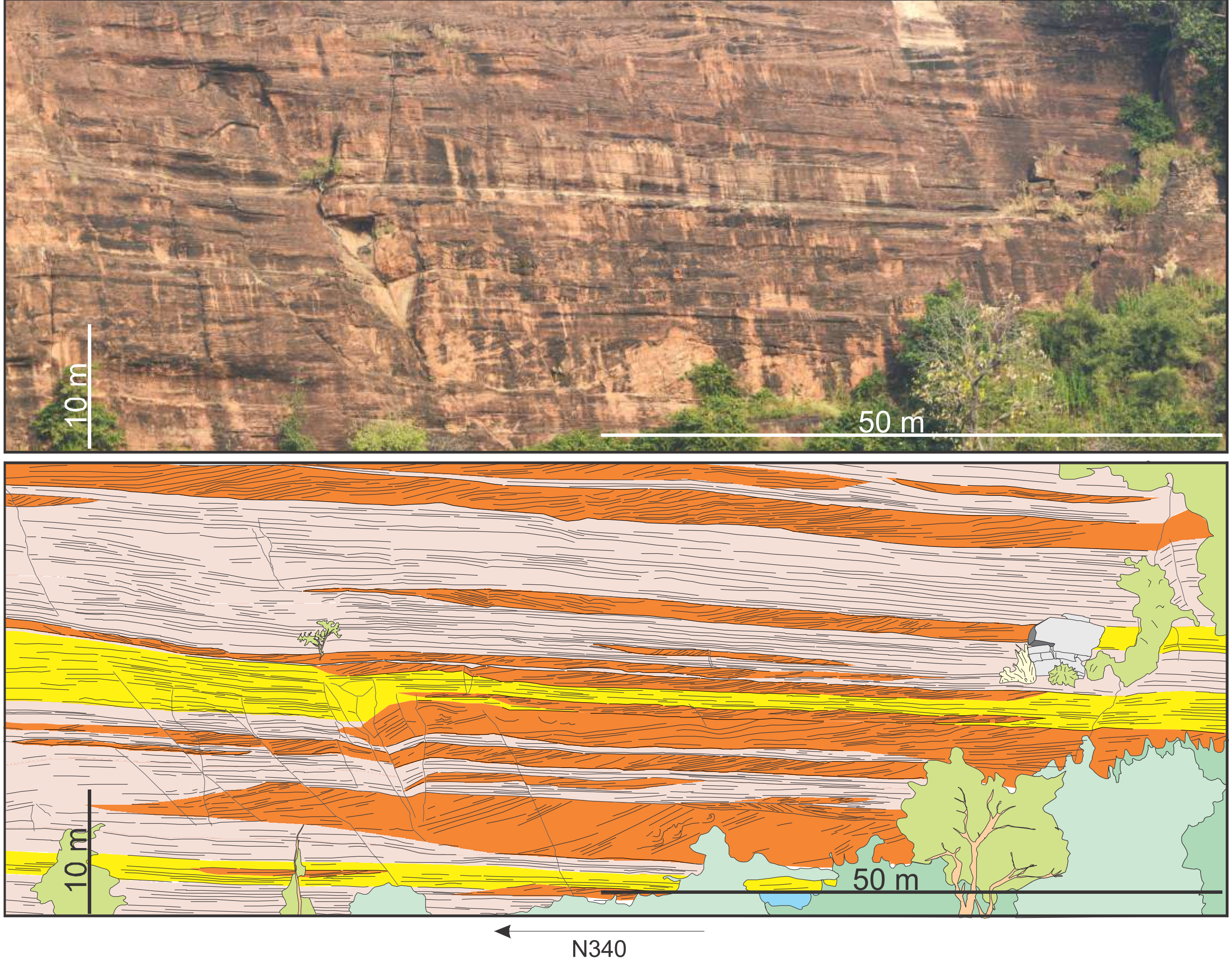

FIGURE 6

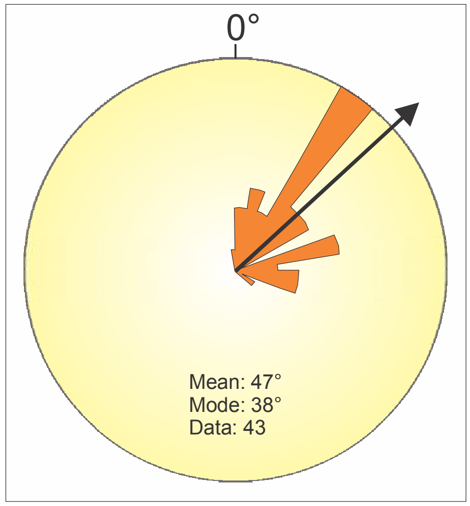

FIGURE 7

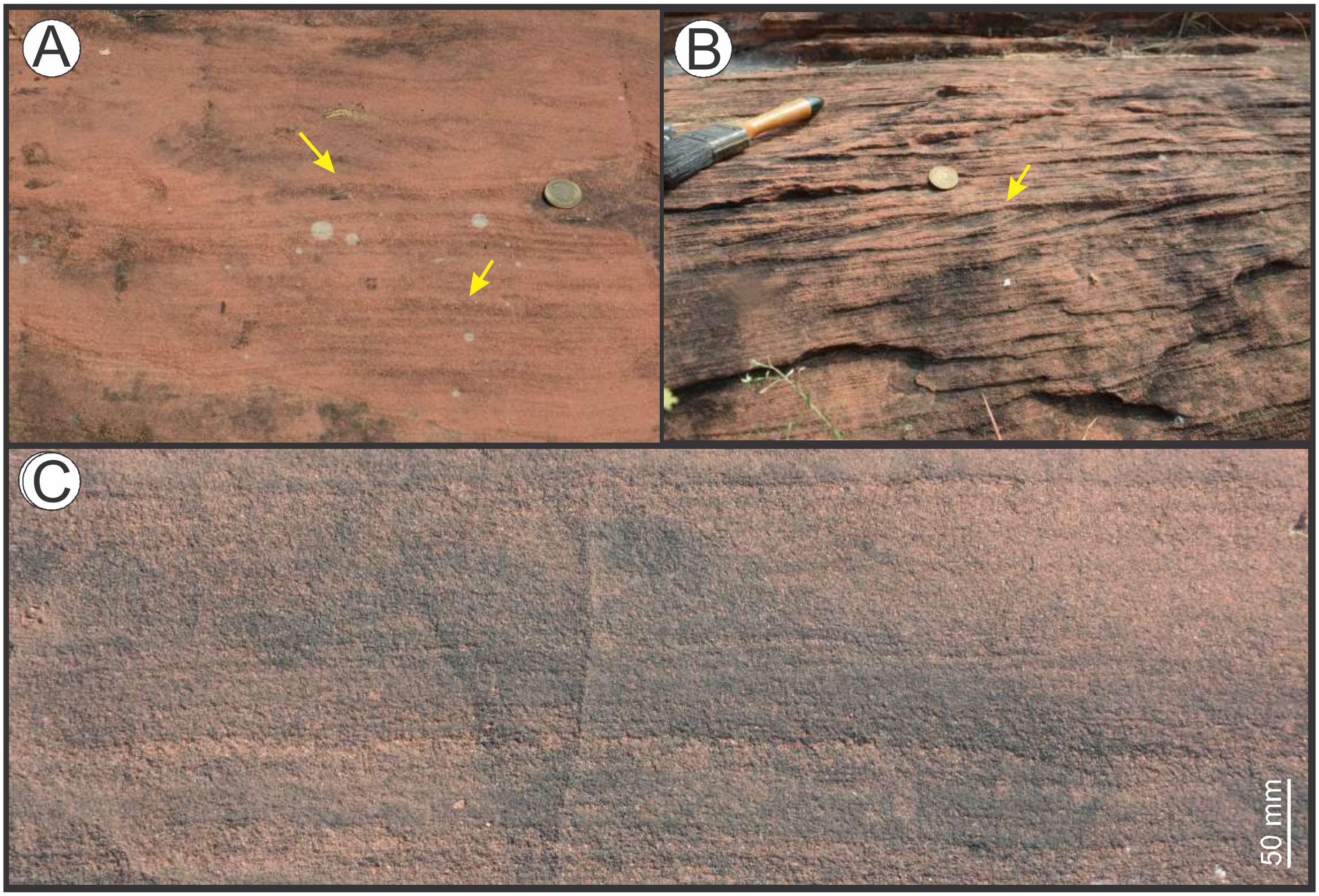

FIGURE 8

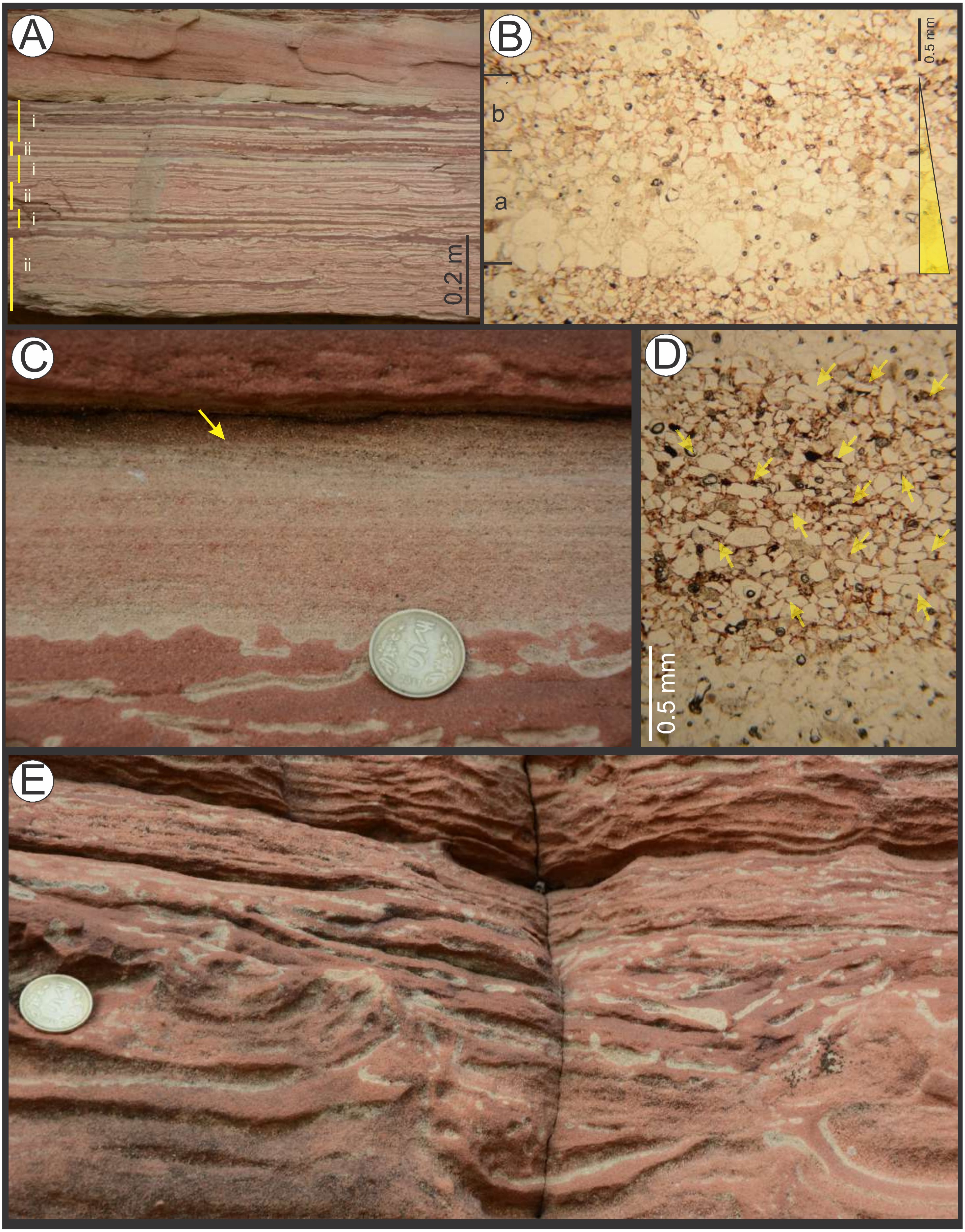

FIGURE 9

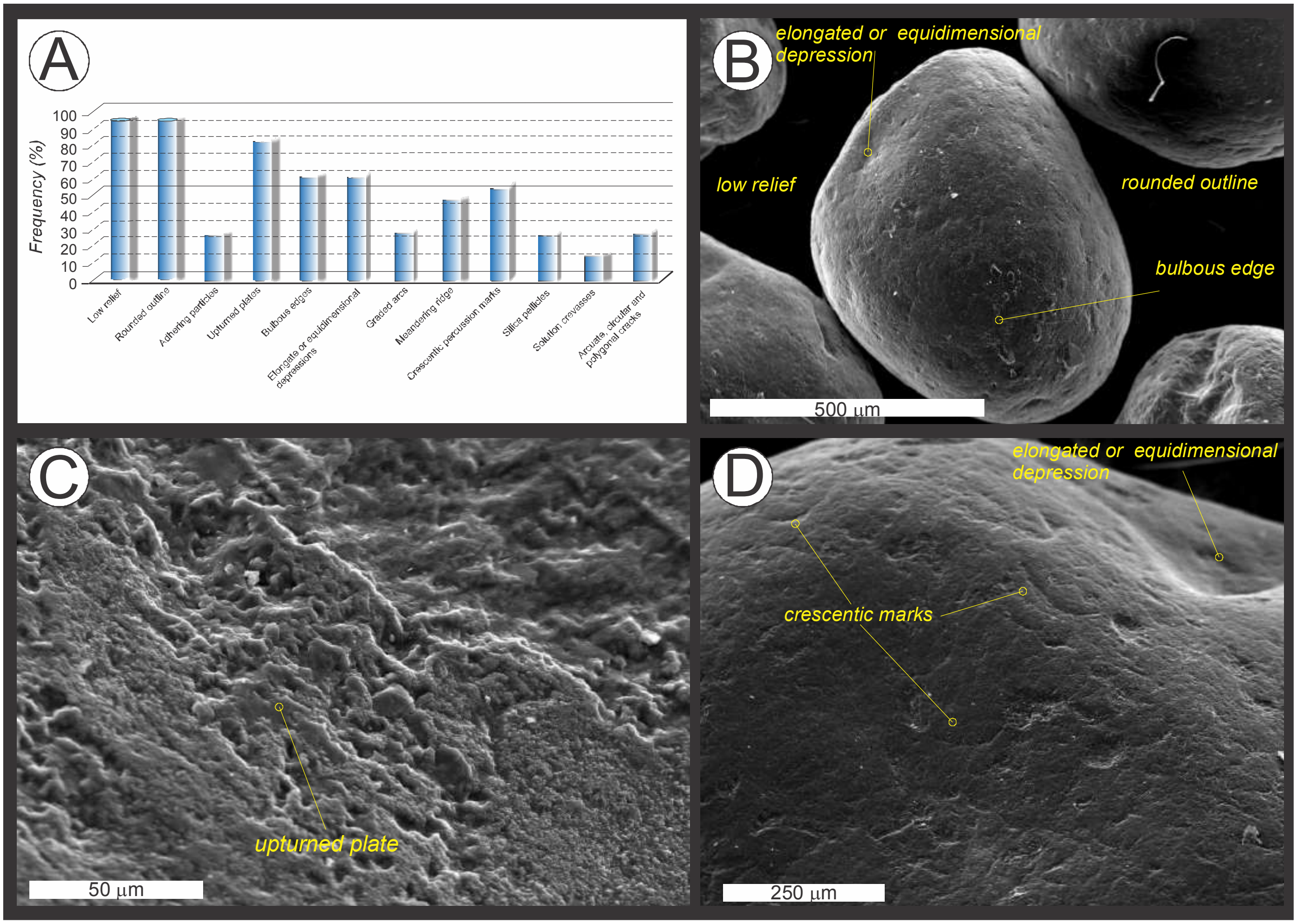
A
Frequency (%)
100
90
80
70
60
50
40
30
20
10
0
Low relief
Rounded outline
Adhering particles
Upturned plates
Bulbous edges
Elongate or equidimensional depressions
Graded arcs
Meandering ridge
Crescentic percussion marks
Silica pellicles
Solution crevasses
Arcuate, circular and polygonal cracks
B
elongated or equidimensional depression
low relief
rounded outline
bulbous edge
500 μm
C
upturned plate
50 μm
D
elongated or equidimensional depression
crescentic marks
250 μm

FIGURE 10

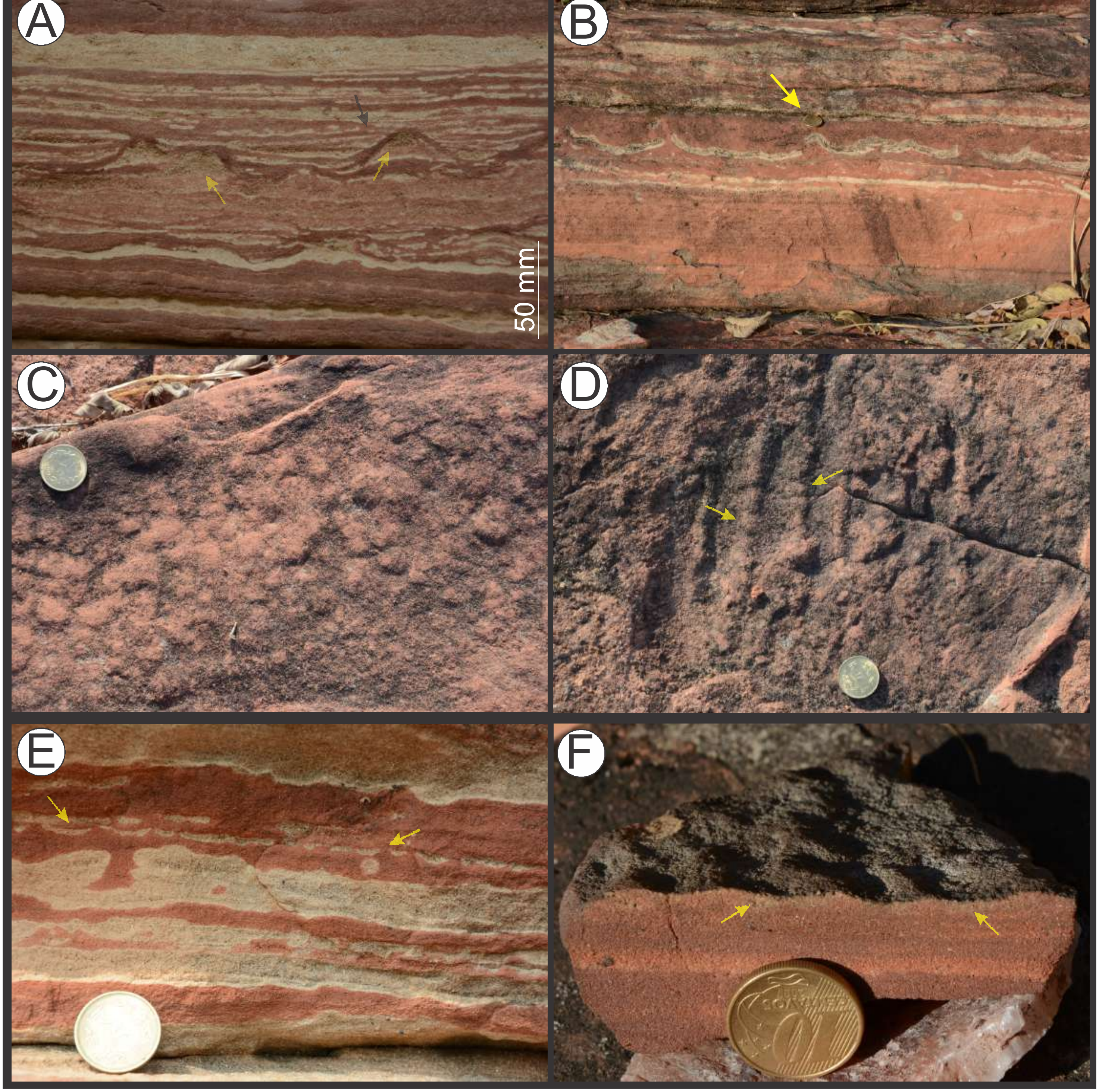

FIGURE 11

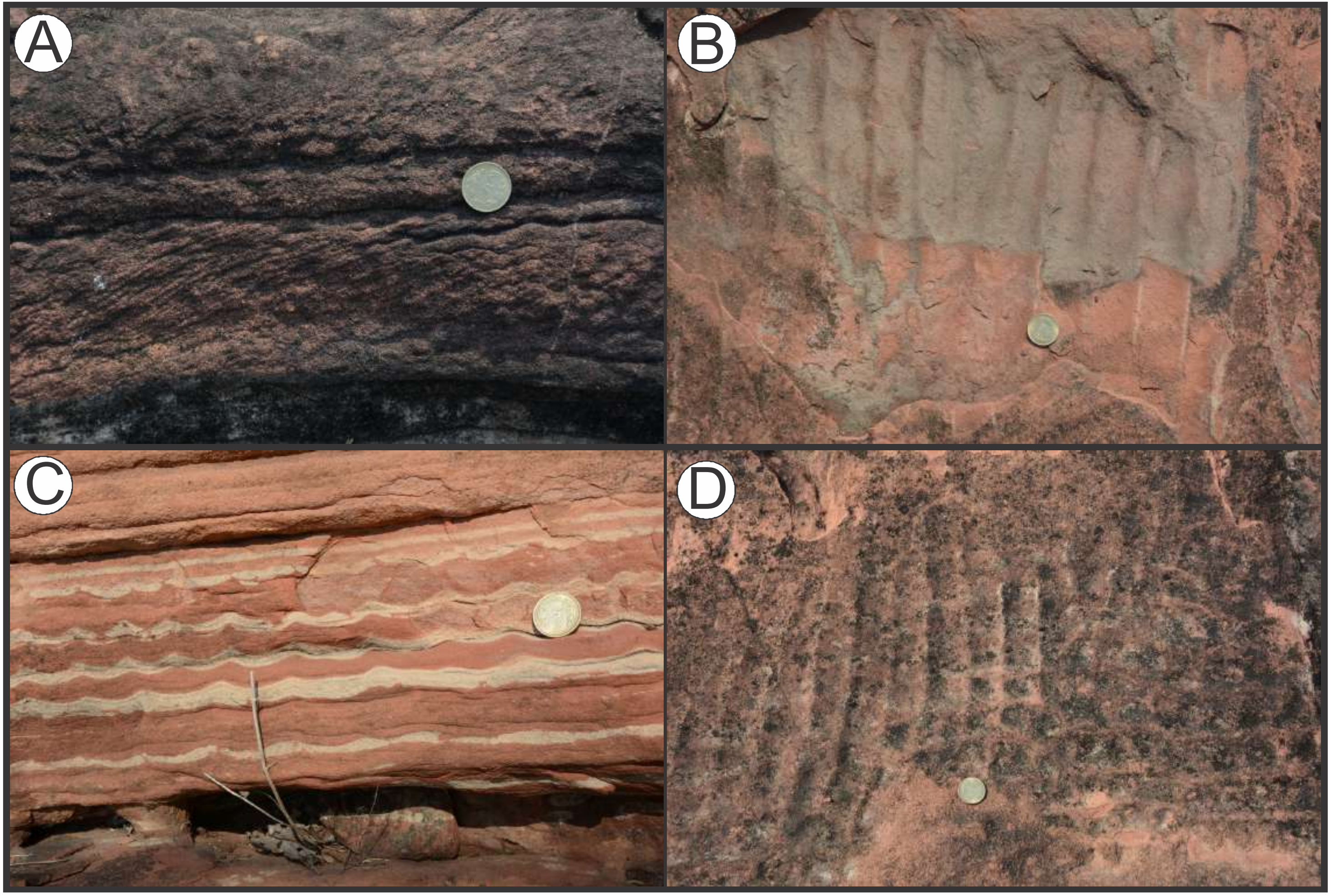

FIGURE 12

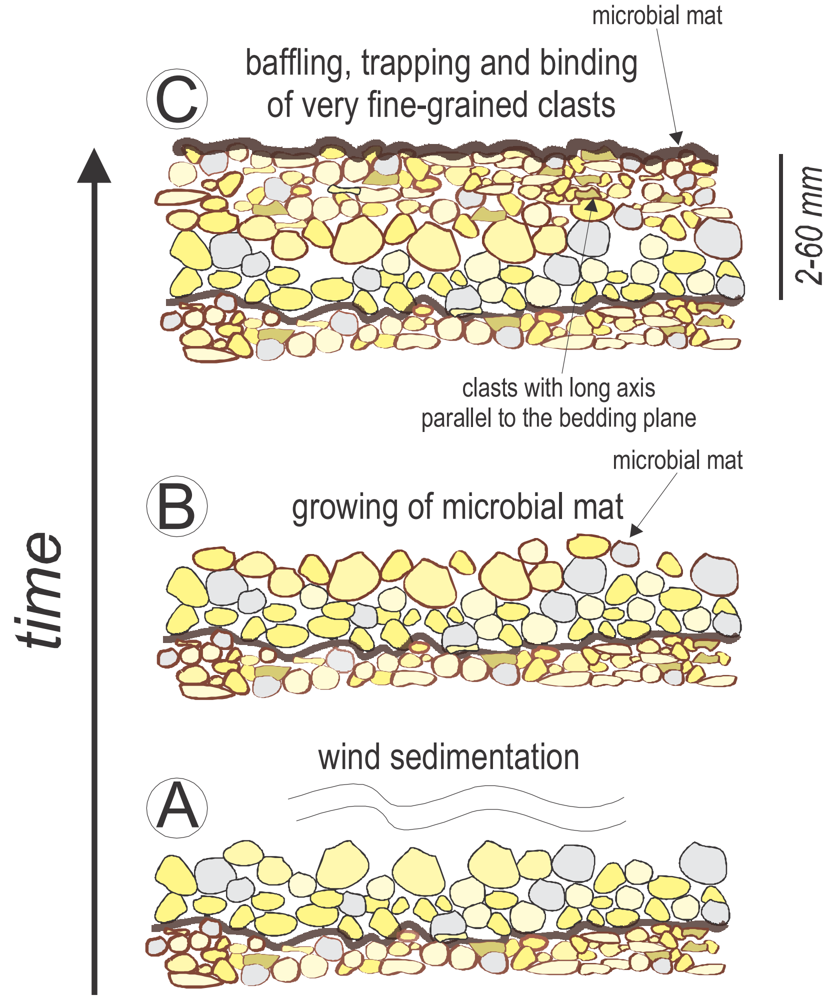
microbial mat
baffling, trapping and binding
of very fine-grained clasts
C
2-60 mm
clasts with long axis
parallel to the bedding plane
microbial mat
B
growing of microbial mat
time
wind sedimentation
A

FIGURE 13

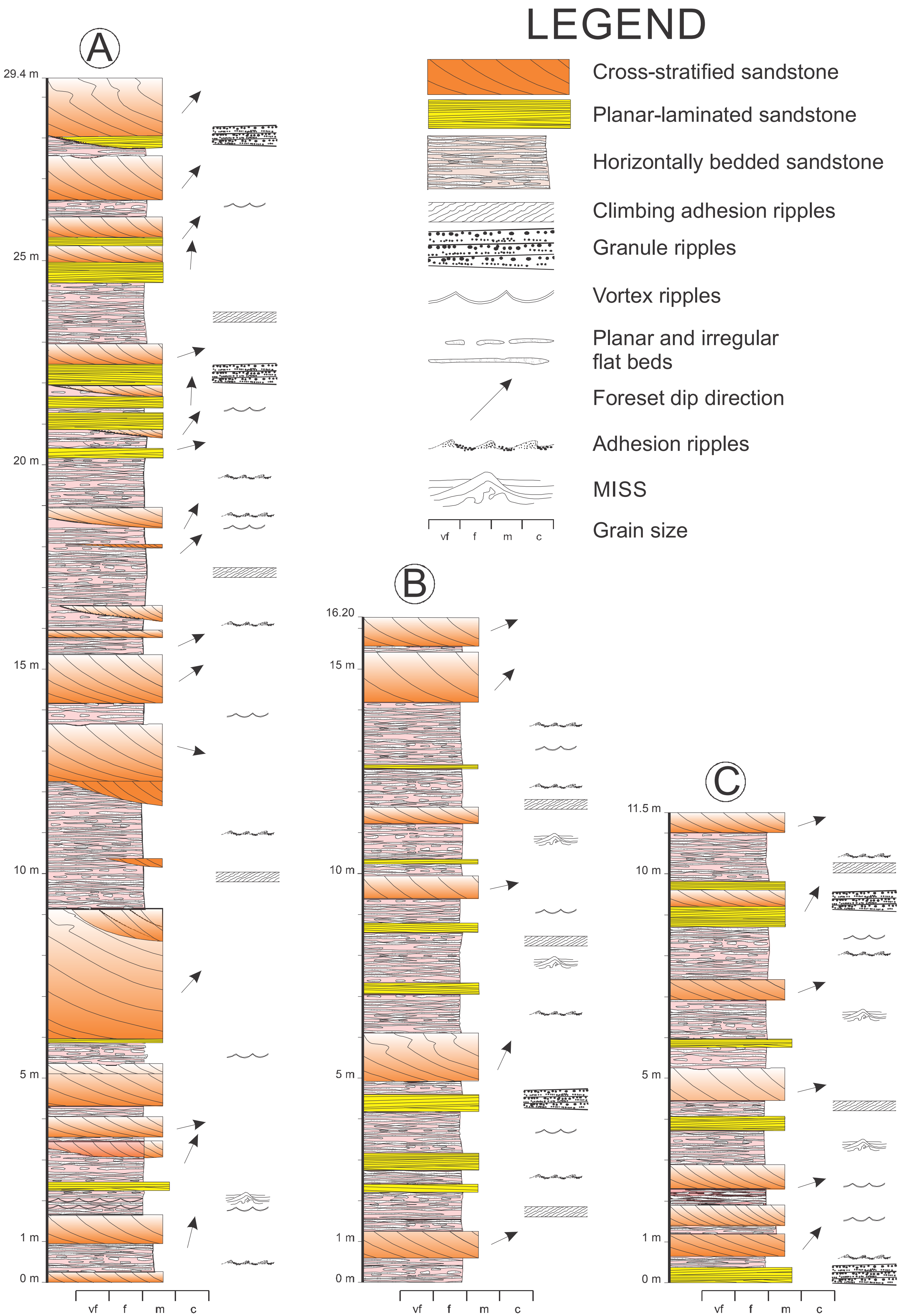
LEGEND
Cross-stratified sandstone
Planar-laminated sandstone
Horizontally bedded sandstone
Climbing adhesion ripples
Granule ripples
Vortex ripples
Planar and irregular flat beds
Foreset dip direction
Adhesion ripples
MISS
Grain size
vf f m c
A
29.4 m
25 m
20 m
15 m
10 m
5 m
1 m
0 m
B
16.20
15 m
10 m
5 m
1 m
0 m
C
11.5 m
10 m
5 m
1 m
0 m

FIGURE 14

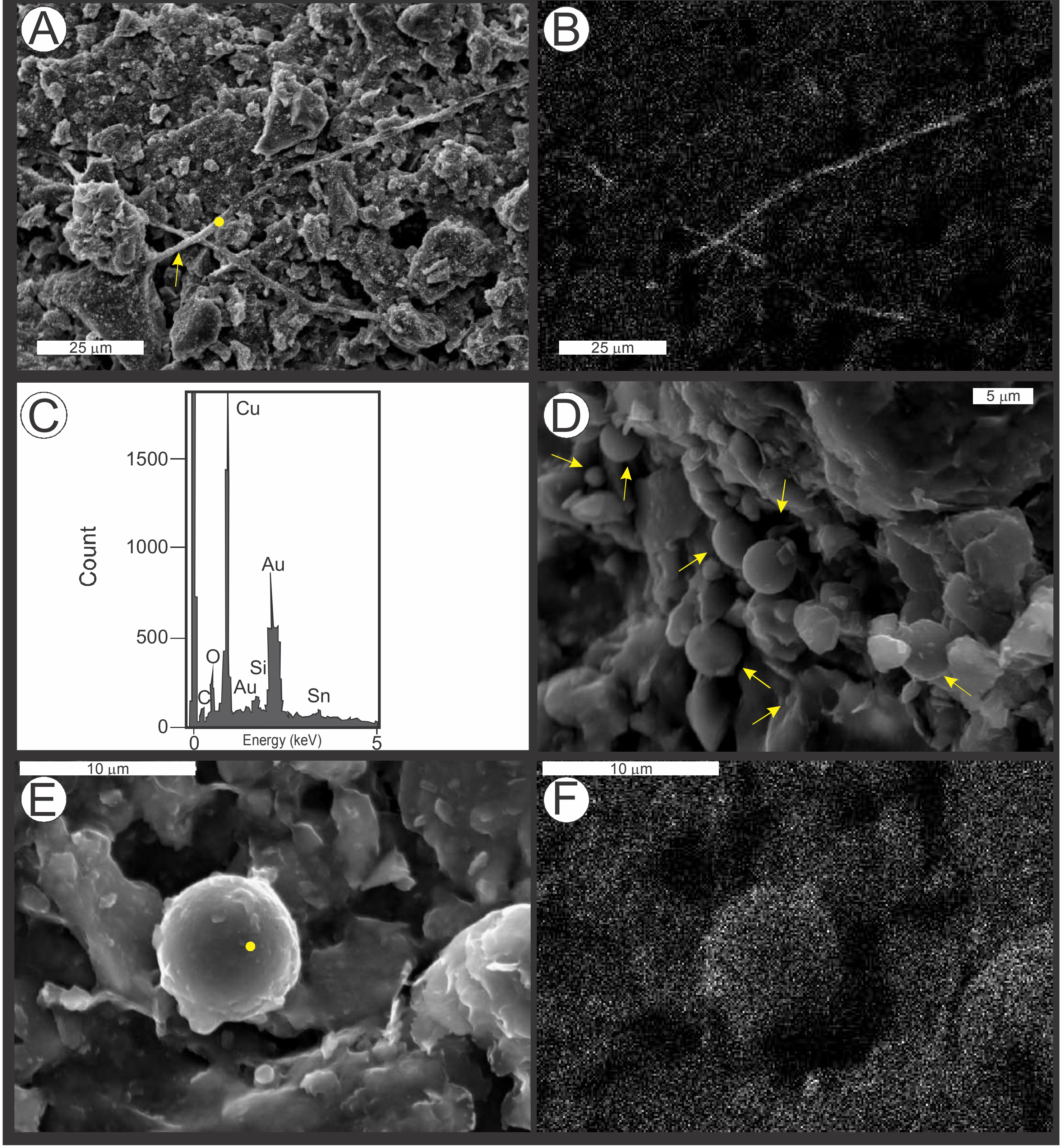
A
25 µm
B
25 µm
C
Count
1500
1000
500
0
Cu
Au
O
Si
Au
C
Sn
0
Energy (keV)
5
D
5 µm
E
10 µm
F
10 µm

FIGURE 15

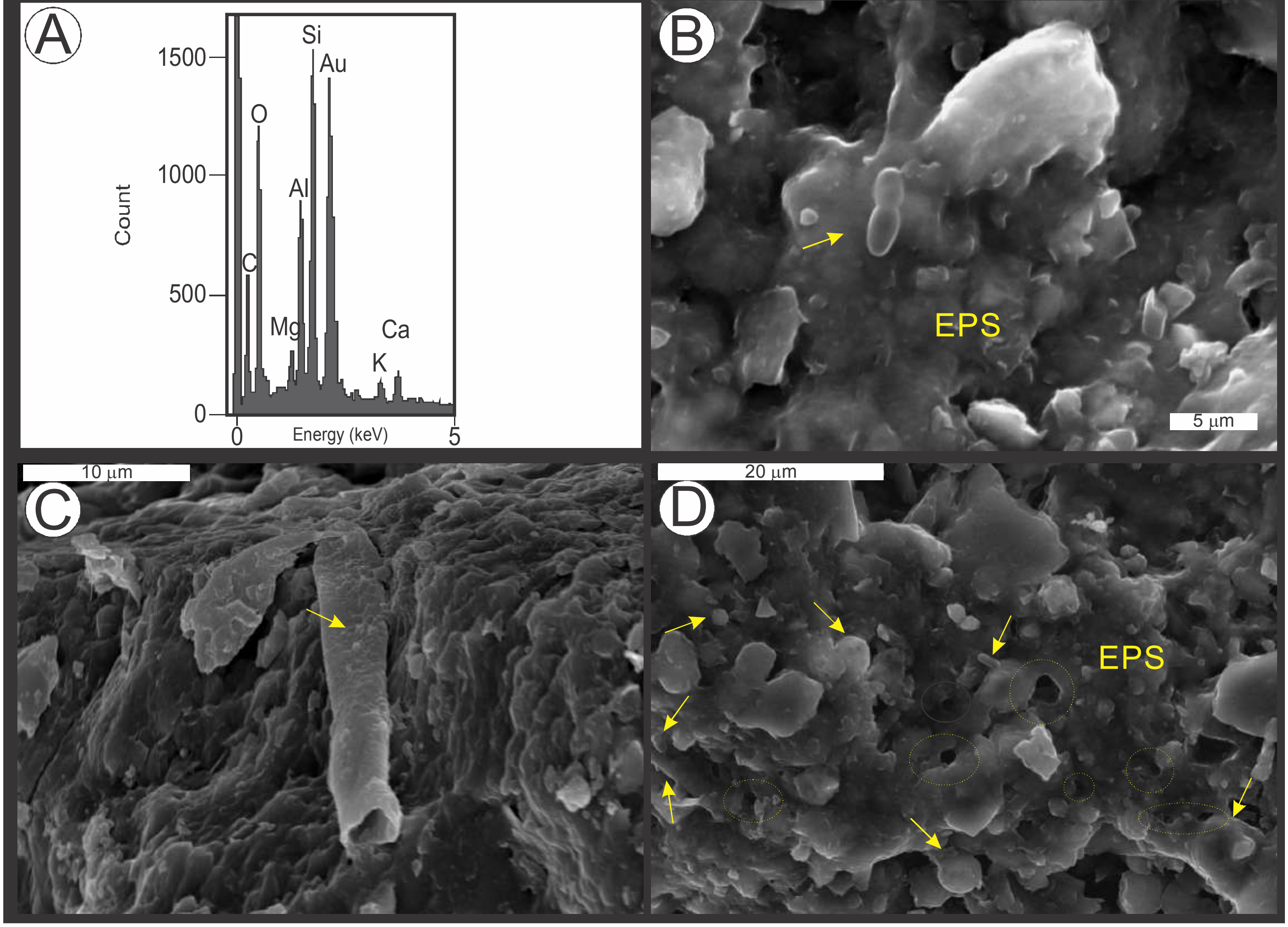
A
Si
Au
1500
O
1000
Al
Count
C
500
Mg
Ca
K
0
0
Energy (keV)
5
B
EPS
5 µm
10 µm
C
20 µm
D
EPS

FIGURE 16

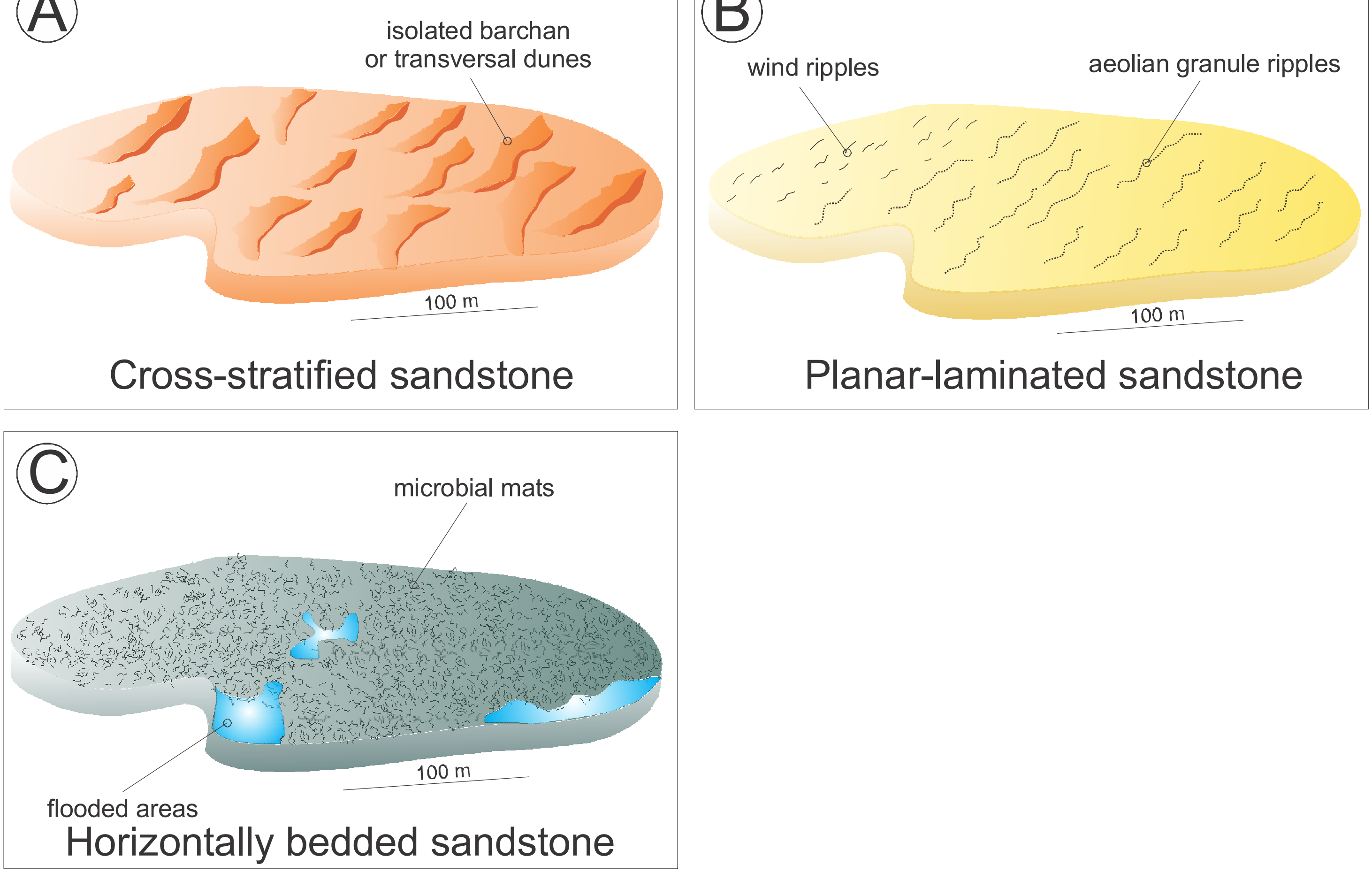
A
isolated barchan
or transversal dunes
100 m
Cross-stratified sandstone
B
wind ripples
aeolian granule ripples
100 m
Planar-laminated sandstone
C
microbial mats
flooded areas
100 m
Horizontally bedded sandstone

FIGURE 17

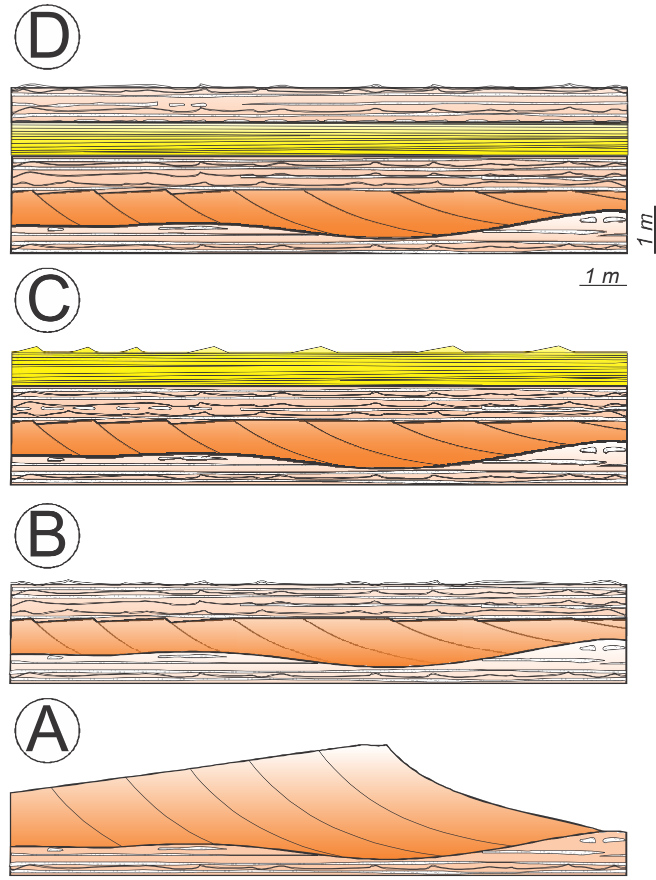

FIGURE 18

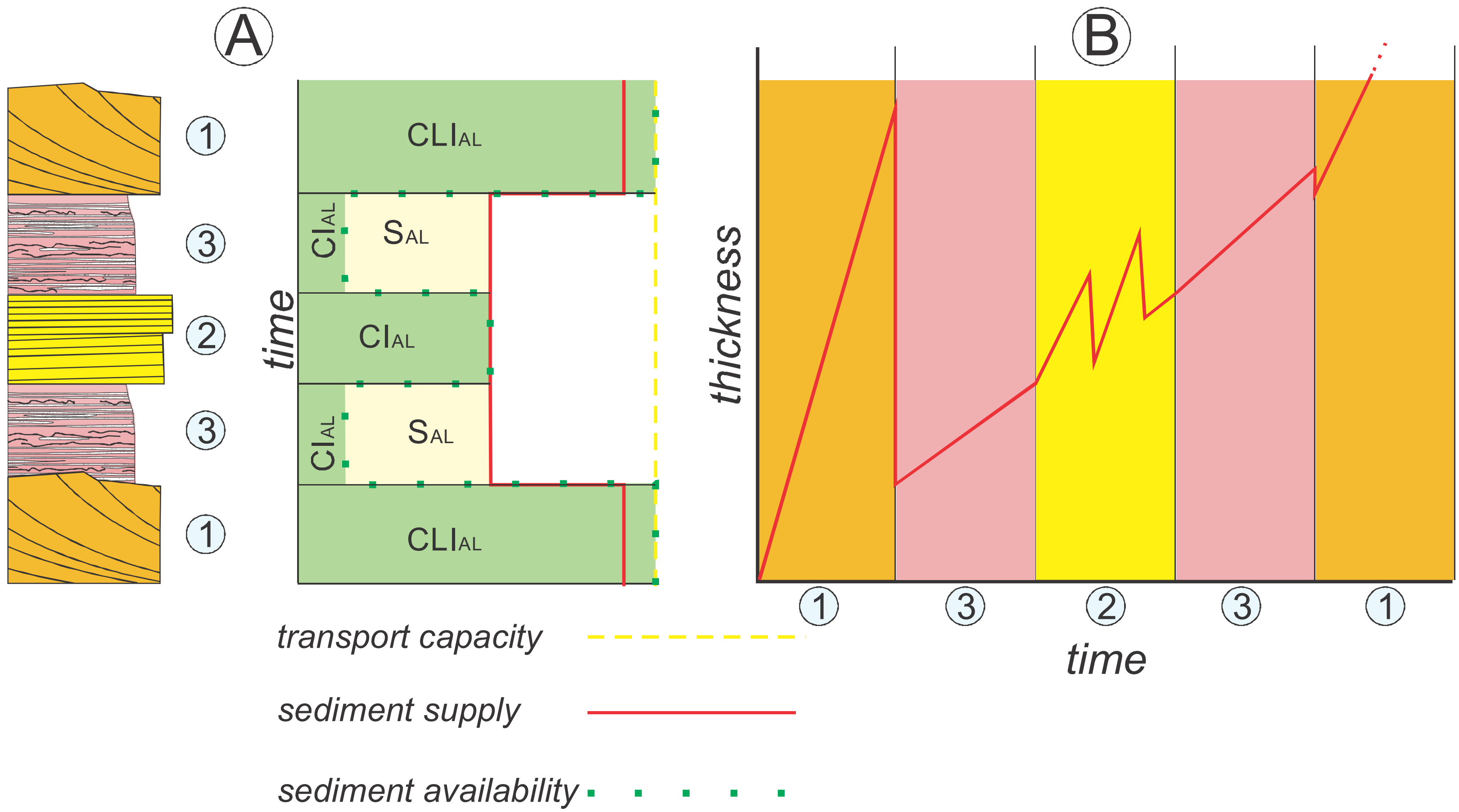
A
B
1
3
2
3
1
CLIAL
CIAL
SAL
CIAL
CIAL
SAL
CLIAL
time
thickness
time
transport capacity
sediment supply
sediment availability

FIGURE 19

Table 1. Petrographic mean composition of 11 samples of fine- and medium-grained sandstone of the three architectural elements. Overall, the sandstone can be classified as sublitharenite.

Fine- and medium-grained sandstone				
Constituents	Quartz	Lithic fragments	Feldspar	Heavy minerals
% distribution	70.3	23.8	5.1	0.8

Table 2. Summary of architectural elements and lithofacies observed in Venkatpur Formation

Architectural element	Lithofacies	Description	Interpretation
Cross-stratified sandstone	Sets of cross-stratifications	Simple sets of cross-stratifications, commonly less than 1 m thick. Foresets laminae have tangential bottom and are prevalently constituted of medium-grained sandstone alternated to fine- and coarse-grained sandstone.	Simple transverse or barchan dunes. Probably, the original dimension of the dunes was not more than 10 m.
Planar-laminated sandstone	Discontinuous, parallel-laminated, medium- to coarse-grained sandstone	Thin discontinuous laminae of medium- and fine-grained grading to coarse- and medium-grained sandstone. Small sets with low-angle cross laminations are occasionally present.	Discontinuous parallel-laminated laminae are interpreted as small granule ripples, whereas sets with cross-laminations suggest large granule ripples (Fryberger et al., 1992).
	Continuous, parallel-laminated, fine- and medium-grained sandstone	Fine- to medium-grained very laterally continuous laminations, occasionally showing inverse grading.	Subcritically climbing translatent strata (Hunter, 1977) produced by climbing wind ripples.
Horizontally bedded sandstone	Planar or irregular flat beddings	Alternating, planar, undulated or contorted, thin layers of white medium- or fine-grained sandstone grading to red fine- or very fine-grained sandstone. Finer portion of the layers show small irregular domes and microfossils remains, attributed to bacteria.	This lithofacies is interpreted as biolaminites (Noffke et al., 1997) formed in a flat temporary damp surface. The medium- or fine-grained layer is deposited by physical aeolian processes; the fine- or very fine-grained layer is formed by baffling, trapping and bonding of wind-driven finer material. Dome forms are interpreted as MISS structure named petee.
	Small planar-concave lens of medium-grained sandstone	Small alternating lens of medium-grained sandstone, embedded by fine-grained sandstone along the same level. On the bed surface they correspond to small asymmetrical ripples.	Small and isolated adhesion ripples.
	Sets with weakly undulated irregular cross-stratifications	Tabular or lenticular sets, 20-70 mm thick, of irregular or weakly undulated cross-stratifications.	Climbing adhesion ripples.
	Symmetrical ripples	In section, climbing symmetrical cross-laminations. On the bed surface, symmetrical ripples with rectilinear and bifurcate crests. Two generation of ripples are commonly observed.	Vortex ripples produced by wind-induced small wave in shallow ponds.

SUPPLEMENTARY 1

The compaction value of the Venkatpur sandstone has been obtained using the formula of the Sheldon & Retallack (2001):

$$C = -S_i/[(F_0/e^{Dk})-1] \quad (1)$$

where, considering the original material as well-sorted and loose quartz sand, $S_i = \rho_d/\rho_s$. ρd = 1,600 kgm^{-3}, which is the maximum bulk density of dry and loose sand (data from web site "The Engineering ToolBox") and ρ_s = 2,660 kgm^{-3} ,which is the density of the quartz, $F_0 = 1-S_i$ is the initial porosity, $k = 0.03e^{4.52F_0}$ is an empirically derived constant. D is the depth in kilometres of the sediment above the Venkatpur Sandstone, which is estimated to be ~4 km. Applying the equation (1) the compaction value (C) is 0.74.

SUPPLEMENTARY 2

The use of the linear wave theory of Airy and the following data (decompacted vortex ripple height [see Supplementary 1], ripple wavelength, vertical form index, and grain size) allow the reconstruction of the ancient wave regime which formed vortex ripples in horizontally bedded sandstone.

The mathematic formula of the linear wave theory of Airy relates wave diameter (d_0) to wave height (H), wave length (L) and water depth (h):

$$d_0 = H/[\sinh(2\pi h/L)] \quad (2)$$

Based on empirical analyses (Miller & Komar, 1984), the wave diameter (d_0) is obtained by:

$$d_0 = \lambda/0.65 \quad (3)$$

where λ is the mean of the wave length of the vortex ripples. In the Venkatpur Sandstone, the mean value of λ is 31.84 mm; thus, d_0 is calculated to be 48.98 mm.

Following the graphic of Allen (1979, his Fig. 1) reporting the relationship between maximum orbital velocity of waves and sediment grain size, the maximum velocity of the waves as a function of the vertical form index can be obtained. Point counting in thin sections of fine grained sandstone with vortex ripples revealed a mean grain diameter of 154 microns. According to the graphic in Allen (1979), the maximum orbital velocities of the waves (U_{max}) varied between 0.14 and 0.26 m/s. The wave period (T) can be calculated by:

$$T = \pi d_o/U_{max} \quad (4)$$

Thus, the maximum wave period (T) is from 0.59 to 1.099 s.

The wave length in deep water (i.e. water depth exceeding the hydrodynamic wave base) is $L_\infty=gT^2/2\pi$. For the two values of T, L_∞= 1.88 m and 0.54 m. The wave length of the waves approaching shoal-water is described by the formula $L= L_\infty[\tanh(2\pi h/L_\infty)]^{1/2}$. Assuming h (water depth) to be in the range between 0.01 m and 50 m, potential values of L at the different attributed water depths can be computed. According to the Airy linear wave theory, $H= d_o \sinh(2\pi h/L)$. Again, the values of H, H/h and H/L can be obtained. The possible values of h can be discriminated by eliminating unrealistic values of H/L and H/h for breaking waves in deep and shallow waters, respectively. Breaking wave limit in water of finite depth is $(H/L)_{lim} = 0.142 \tanh(2\pi h/L)$ (Miche, 1944). In progressively shallower water, the wave breaks when the value H/h exceeds 0.88 (i.e., $(H/h)_{lim} = 0.88$) (McCowan, 1894; Allen, 1984). Finally, considering two values of L_∞, likely values of water depth for the vortex ripple formation in Venkatpur Sandstone are obtained. These values are 0.2-0.5 m for T=1.099 s and 0.04-0.5 m for T=0.59 s.